Marine Environmental Research 220 (2026) 108123

Contents lists available at ScienceDirect

Marine Environmental Research

journal homepage: www.elsevier.com/locate/marenvrev

Stable isotope insights into the habitat use of two benthic invertebrates along Antarctic glacier-influenced fjords

Pau Bardi-Puigdefàbregas [a,b,*], Miguel Bascur [a,b,*], David K.A. Barnes [c], Stuart Jenkins [d], Carlos P. Muñoz-Ramírez [e], Estefanía Rodríguez [f], Antonio Brante [g,h], Luis Cardona [a,b], Conxita Avila [a,b]

[a] Departament de Biologia Evolutiva, Ecologia i Ciències Ambientals, Facultat de Biologia, Universitat de Barcelona, Av. Diagonal 643, 08028, Barcelona, Catalonia, Spain
[b] Institut de Recerca de la Biodiversitat, Facultat de Biologia, Universitat de Barcelona, Av. Diagonal 643, 08028, Barcelona, Catalonia, Spain
[c] British Antarctic Survey, Madingley Road, Cambridge, CB3 0ET, United Kingdom
[d] School of Ocean Sciences, Bangor University, Askew St, Menai Bridge LL59 5AB, Bangor, United Kingdom
[e] Instituto de Entomología, Universidad Metropolitana de Ciencias de la Educación, Av. José Pedro Alessandri 774, Santiago, Chile
[f] Division of Invertebrate Zoology, American Museum of Natural History, Central Park West at 79th Street, New York, NY, 10024, United States of America
[g] Departamento de Ecología, Facultad de Ciencias, Universidad Católica de la Santísima Concepción, Av. Alonso de Ribera 2850, Concepción, Chile
[h] Centro de Investigación en Biodiversidad y Ambientes Sustentables, Universidad Católica de la Santísima Concepción, Av. Alonso de Ribera 2850, Concepción, Chile

ARTICLE INFO

Keywords:
Glacier retreat
Climate change
Western Antarctic Peninsula
Land-terminating glacier
Marine-terminating glacier
Soft-bottom macrofauna
Trophic ecology

ABSTRACT

Retreating glaciers are rapidly transforming fjord ecosystems along the Western Antarctic Peninsula (WAP), yet the trophic responses of benthic fauna remain poorly understood. We analysed $\delta^{13}C$, $\delta^{15}N$, $\delta^{34}S$, and C:N ratios in two soft-bottom species collected along distance gradients from retreating glaciers in two WAP fjords. The study included the deposit-feeding bivalve *Nuculana inaequisculpta* from Marian Cove (King George Island) and the opportunistic-feeding sea anemone *Edwardsia* sp. from Sheldon Cove (Adelaide Island). Near the land-terminating glacier at Marian Cove, bivalves were depleted in ^{13}C, consistent with reduced phytoplankton growth under surface meltwater influence. Near the marine-terminating glacier at Sheldon Cove, anemones were ^{13}C-enriched, in line with enhanced phytoplankton blooms driven by deep meltwater inflow. $\delta^{15}N$, $\delta^{34}S$, and C:N ratios showed no fjord-scale trends and appeared governed by local factors. Low $\delta^{34}S$ values reflected suboxic sediment inputs in both fjords, possibly linked to denitrification and elevated $\delta^{15}N$ baselines. When associated with blooms, anemones appeared to rely less on sedimentary sources while bivalves showed signs of sediment hypoxia. In both species, reliance on suboxic sediments was potentially related to poor nutritional condition. Environmental factors linked to submarine sills may have improved bivalve nutritional condition and increased anemone trophic level. Overall, benthic $\delta^{34}S$ emerged as an excellent indicator in Antarctic marine habitats, and $\delta^{13}C$ could be a tracer of productivity associated with glacier configuration in Antarctic fjords. Local meltwater conditions may limit organic matter flux to the benthos, nuancing the role of newly ice-free areas as carbon sinks within a negative climate feedback.

1. Introduction

Antarctic marine ecosystems have historically been among the most environmentally constant surface habitats on the planet (Stark et al., 2019). However, the Western Antarctic Peninsula (WAP) is now particularly vulnerable to global physical changes (Klages et al., 2024) and among the fastest-warming regions on Earth (Convey and Peck, 2019; Siegert et al., 2019; Wang et al., 2025). In the WAP, almost 90% of glaciers are now retreating, and their retreat rates continue to increase as ocean temperatures rise (Cook et al., 2016). When glaciers retreat,

* Corresponding authors. Departament de Biologia Evolutiva, Ecologia i Ciències Ambientals, and Institut de Recerca de la Biodiversitat, Facultat de Biologia, Universitat de Barcelona, Av. Diagonal 643, 08028, Barcelona, Catalonia, Spain.
E-mail addresses: pau.bardi@gmail.com (P. Bardi-Puigdefàbregas), mbascuba7@alumnes.ub.edu (M. Bascur), dkab@bas.ac.uk (D.K.A. Barnes), s.jenkins@bangor.ac.uk (S. Jenkins), car.munozramirez@gmail.com (C.P. Muñoz-Ramírez), erodriguez@amnh.org (E. Rodríguez), abrante@ucsc.cl (A. Brante), luis.cardona@ub.edu (L. Cardona), conxita.avila@ub.edu (C. Avila).

https://doi.org/10.1016/j.marenvres.2026.108123
Received 12 November 2025; Received in revised form 24 April 2026; Accepted 14 May 2026
Available online 15 May 2026

they calve icebergs (Holdsworth and Glynn, 1981; Alley et al., 2023). This leads to new fjordic habitats, biota colonisation, and potential carbon sink areas (Barnes et al., 2020). Eventually, glaciers can lose contact with the ocean and transition into land-terminating systems, leading to profound changes in the physical and biogeochemical characteristics of fjords (Jones et al., 2023). Land-terminating glaciers have been proposed to locally reduce primary productivity by forming a turbid surface plume that stratifies the water column and limits light penetration (Kim et al., 2021; Demidov et al., 2023; Hoshiba et al., 2024).

Iron is an essential micronutrient for phytoplankton, but it is poorly soluble in seawater and represents the main limiting nutrient in the open waters of the Southern Ocean (Moore et al., 2013; Ryan-Keogh et al., 2017). However, retreating glaciers release large amounts of iron (Annett et al., 2015; Hodson et al., 2017), promoting strong phytoplankton blooms at nearshore environments such as fjords (Alderkamp et al., 2012; Bown et al., 2017; Bae et al., 2021). In these ecosystems, glacial meltwater can provide sufficient iron to overcome its limitation on phytoplankton growth. This shifts the main controls on productivity to other environmental factors, such as those driven by land-terminating glaciers.

Any change in the quantity or quality of organic matter exported to the seafloor may affect benthic life (Lee et al., 2025). The Antarctic benthos occupies multiple trophic levels (Thrush et al., 2021) and plays a key role in benthic-pelagic coupling (Elias-Piera, 2015; Alurralde et al., 2019; Jędruch et al., 2025). It also contributes to long-term carbon sequestration by burying refractory organic matter (Barnes, 2017; Barnes and Sands, 2017), a process that creates a negative —mitigating— feedback loop with climate change (Peck et al., 2010; Zwerschke et al., 2022). Although fjordic seafloor habitats can be hotspots of biodiversity and carbon sequestration (Grange and Smith, 2013; Smith et al., 2015; Barnes et al., 2020), benthic responses to glacier retreat are largely unexplored to date. However, Antarctica's stable environment, combined with the typically slow growth of its inhabitants and low population turnover rates (Clarke et al., 2007), provides an excellent scenario for detecting glacial-driven benthic shifts (Sahade et al., 2015).

Stable isotope analysis has become one of the most important advances in trophic ecology in recent decades (Schwartz et al., 2014). Since stable isotope ratios in consumer tissues reflect those of their diet, they have been widely used as proxies for inferring food sources over mid to long-term time periods (Peterson and Fry, 1987; Dalerum and Angerbjörn, 2005). Therefore, stable isotopes can help study trophic relationships and foraging habitat use in marine ecosystems (Dunton, 2001; Boecklen et al., 2011; Choy et al., 2011; Amiraux et al., 2023; Iken et al., 2023; Oleszczuk et al., 2023). However, stable isotope analysis also faces challenges, such as the difficulty in establishing reliable reference values from which to assess isotopic enrichment or depletion, as baselines fluctuate across space and time (Ortiz et al., 2024). Among the most widely used ones, the carbon stable isotope ratio ($\delta^{13}C$) plays a crucial role in identifying the primary sources of carbon (Peterson and Fry, 1987). The nitrogen stable isotope ratio ($\delta^{15}N$), in turn, is useful for evaluating an organism's trophic level (Vander Zanden and Rasmussen, 1999), while the sulphur stable isotope ratio ($\delta^{34}S$) may serve to detect the influence of sedimentary redox processes (Peterson, 1999; Raoult et al., 2024). Additional metrics, such as the carbon-to-nitrogen (C:N) ratio, can provide complementary ecological insights. The C:N ratio is commonly used in marine animals as a proxy for relative lipid content because lipids are carbon-rich and nitrogen-poor (Post et al., 2007). Accordingly, higher C:N values indicate greater lipidic energy reserves and, therefore, better nutritional condition. In this context, nutritional condition is defined as the relative amount of lipid-based stored energy in the tissues (Bascur et al., 2020). Together, these tools have proven valuable for understanding habitat use and nutritional condition in marine ecosystems (Mincks et al., 2008; Seyboth et al., 2018; Cani et al., 2025). Nevertheless, only three recent studies have examined glacier-driven isotopic variation in benthic invertebrates from Antarctic fjords (Alurralde et al., 2020; Jędruch et al., 2025; Lee et al., 2025). These works are restricted to intertidal or shallow subtidal areas, leaving deeper fjord habitats (i.e., most of the fjord's space for life) unexplored by this technique.

Among Antarctic benthic invertebrates, the present study focuses on two ecologically relevant soft-bottom infaunal species from different phyla and with different trophic strategies. Both are highly abundant in Antarctic fjords and play a role in carbon pathways to sequestration (Lovell and Trego, 2003). As secondary producers, both are also valuable indicators of shifts at the base of food webs in glacier-influenced systems. The bivalve mollusc *Nuculana inaequisculpta* (Lamy, 1906) (Nuculanida: Nuculanidae) is a small protobranch (up to 17 mm of shell length) with a patchy circumantarctic distribution, recorded at depths down to 810 m (Cattaneo-Vietti et al., 2000; Gordillo et al., 2017). It inhabits muddy benthic environments and feeds on sedimentary organic matter (Zardus, 2002). The second study species is an anthozoan cnidarian from the genus *Edwardsia* (Quatrefages, 1842) (Actiniaria: Edwardsiidae). This is a diverse group that includes 64 described species distributed worldwide (Rodríguez et al., 2025), of which three are present in Antarctica (Sanamyan et al., 2015). Edwardsiid sea anemones are opportunistic feeders, ranging from carnivory to suspension feeding. They burrow in the soft sediment and extend their tentacle crown into the water column to capture suspended organic particles or prey (Daly et al., 2012; Rodríguez et al., 2014). Our focal species thus provide complementary perspectives for evaluating marine benthic trophic responses to glacier retreat.

In the present work, we measured $\delta^{13}C$, $\delta^{15}N$, $\delta^{34}S$, and C:N ratios of these species from Antarctic shallow-shelf (86–500 m) soft-bottom fjord transects affected by glacier retreat. The study was conducted in two distinct WAP systems: Marian Cove, influenced by a land-terminating glacier, and Sheldon Cove, influenced by a marine-terminating glacier. We also integrated measurements of fluorescence (as a proxy of chlorophyll *a*) and dissolved oxygen availability along the fjords, providing additional context on environmental conditions. Furthermore, we analysed the local effects of seabed morphology on the ecology and nutritional condition of both study species. Through this approach, we aimed to assess how glacier retreat-driven environmental gradients and seabed features shape the trophic ecology of two benthic invertebrates in Antarctic soft-bottom fjords under rapid environmental change.

2. Materials and methods

2.1. Sample collection

This study used specimens collected during the ICEBERGS II research cruise in December 2018 (JR18003; British Antarctic Survey) on the RRS James Clark Ross along the WAP (Fig. 1A). Samples were obtained from the sedimentary fjords Marian Cove (King George Island, South Shetland Islands, 62.2 °S; Fig. 1B) and Sheldon Cove (Adelaide Island, 67.3 °S; Fig. 1C), at five stations within each fjord. These two systems differ in glacier configuration. Although at the time of sampling the glacier in Marian Cove still had a small area terminating in the sea, most of its surface already ended on land. Therefore, we consider Marian Cove as influenced by a land-terminating glacier (Jones et al., 2023). Meanwhile, Sheldon Cove is fully influenced by a marine-terminating glacier. Each target species was analysed within the fjord where it was collected, in order to assess stable isotope variation along the gradient associated with glacier retreat within each fjord. The specimens of the bivalve *Nuculana inaequisculpta* were obtained from Marian Cove, and those of the sea anemone *Edwardsia* sp. were collected from Sheldon Cove.

The sampled stations followed a gradient of glacial influence, including shallow-shelf areas from the fjord mouth (free of ice since the beginning of records) to the glacier terminus (recently ice-free). Therefore, the stations represent a continuum of historical glacier coverage, ranging from areas that have been uncovered since the last

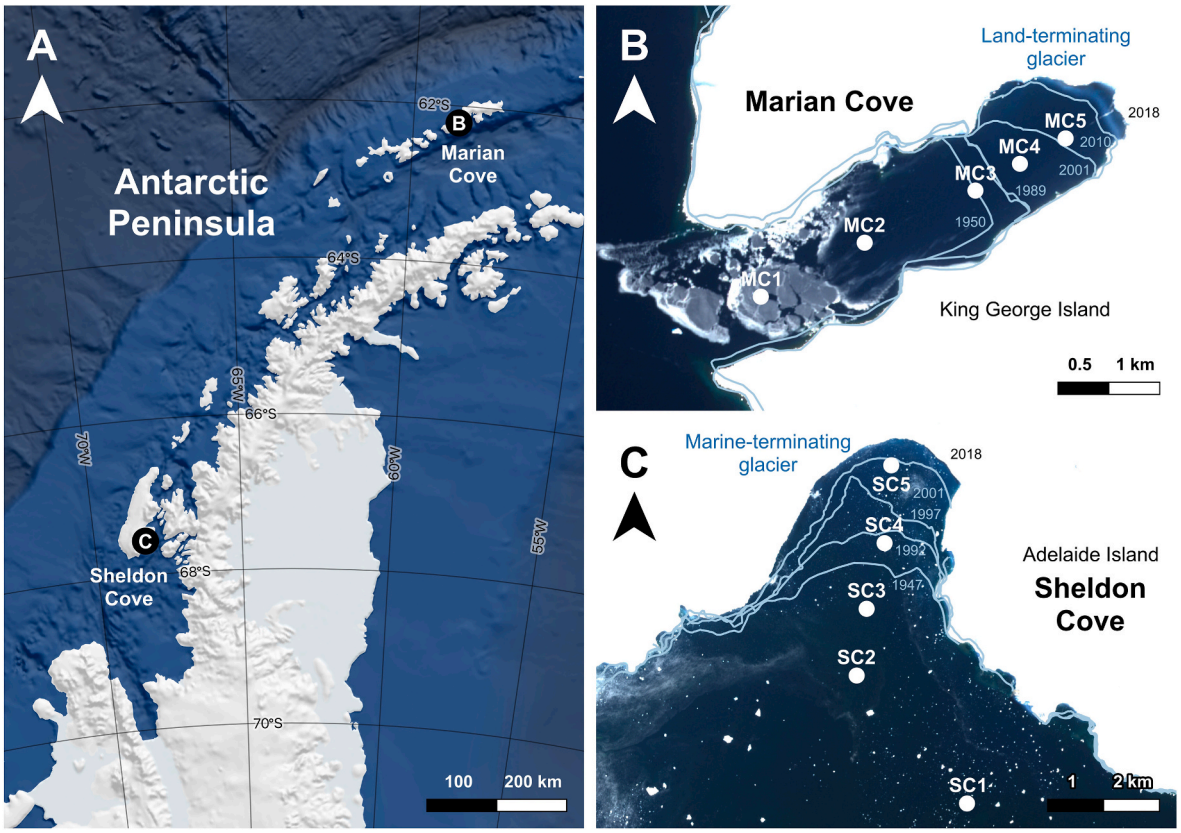

Fig. 1. Location of the study areas and sampling stations in Marian Cove and Sheldon Cove (WAP). Map of the Western Antarctic Peninsula (A), showing the location of Marian Cove in King George Island (B) and Sheldon Cove in Adelaide Island (C). Maps (B) and (C) show the sampling stations (MC1–MC5 and SC1–SC5, respectively) and the estimated historical glacier retreat lines (unpublished data from the Mapping and Geographic Information Centre, British Antarctic Survey). Basemap in (A) was generated in QGIS (v3.44.2; www.qgis.org) using the *Quantarctica* package (v3.2). (B) and (C) use Sentinel-2 basemaps from the Copernicus Open Access Hub, taken on 13 October 2019 and 18 January 2020, respectively. All maps were annotated using QGIS.

glacial maximum to others that became ice-free during the last decades (Zwerschke et al., 2022). Sampling stations ranged from 86 to 111 m depth in Marian Cove (MC1–MC5) and from 175 to 500 m in Sheldon Cove (SC1–SC5; Table S1). The transects encompassed prominent submarine sills identified by onboard bathymetric surveys at ca. 107 m depth in Marian Cove (at MC3) and ca. 175 m in Sheldon Cove (at SC2; Sands et al., 2018). Note that the station referred to as SC6 in the cruise report (Sands et al., 2018) is designated here as SC5 for clarity.

At each station, five replicate samples were obtained using a Hamon grab (20 × 40 × 40 cm bucket). Once each successful grab arrived at the vessel deck, it was rinsed over a 1 mm sieve with natural seawater to remove the sediment. When samples were free of sediment, they were sorted into large taxonomic units (e.g., class) and independently stored in pre-labelled bottles with absolute ethanol in the vessel laboratory. All samples were stored at −20 °C until analysis.

Fluorescence (as a proxy of chlorophyll *a* concentration) and dissolved oxygen data were obtained at each sampling station (Table S2) using a SeaBird 911plus CTD (www.seabird.com) installed on the RRS James Clark Ross. Raw profiles were processed with Sea-Bird Data Processing and subsequently averaged at nominal 2 dbar (ca. 2 m) depth bins, following the standard protocol described in the cruise report (Sands et al., 2018). For fluorescence, we identified the peak value within each station profile and selected the set of binned values spanning the 10 m depth window containing the peak, yielding six values per station ($n = 6$). Peak depths ranged from 5 to 15 m in Marian Cove and from 21 to 36 m in Sheldon Cove. For dissolved oxygen, we extracted the deepest 10 m of each profile, yielding six binned values per station ($n = 6$) representative of near-bottom conditions in the vicinity of biological collections. Dissolved oxygen concentrations were originally obtained in μmol kg^{-1} and subsequently converted to mg L^{-1} using the molar mass of O_2 and seawater density estimated from temperature and salinity.

2.2. Study species identification

Specimens of *N. inaequisculpta* were identified based on external morphological characteristics and the help of relevant literature (Engl, 2012; Zettler and Bick, 2025). Regarding *Edwardsia* sp. individuals, they were identified to the genus level after examination of external and internal traits. These *Edwardsia* sp. specimens belong to a species new to science, and some individuals were preserved for taxonomic description, which will be published in a forthcoming study.

Although cryptic diversity has been reported in several Antarctic bivalves (e.g., Linse et al., 2007; Levicoy et al., 2021), *N. inaequisculpta* individuals from Marian Cove belong to a single genetic population (Muñoz-Ramírez et al., 2021). Therefore, in this case, a potential bias arising from comparing unknown different species is minimal. Similarly, the anemone specimens were rigorously morphologically examined, and species-level consistency across samples was ensured. This homogeneity is in line with the relatively recent colonisation of the inner fjords by the populations from the fjord mouth (Zwerschke et al., 2022).

2.3. Specimen dissection and tissue encapsulation

Once at the Universitat de Barcelona, ten specimens per station and species were selected and dissected to extract a specific tissue for subsequent stable isotope analysis (except for SC1, where only five anemones were found). This step was necessary because isotopic signals may

vary across tissues within the same organism (e.g., Yakovis et al., 2012).

The foot tissue of bivalves was selected and isolated for analysis. Muscle tissue is commonly used in animal stable isotope studies (Boecklen et al., 2011) and in bivalves (Yakovis et al., 2012). Although whole-body homogenates are more frequently used (Yakovis et al., 2012), foot tissue avoids contamination from gut contents. Adductor muscles were excluded, as Yakovis et al. (2012) demonstrated that their isotopic composition can differ from that of the foot in the bivalve *Modiolus modiolus*. Moreover, as *N. inaequisculpta* is a very small animal, the adductor muscles could not be used alone due to their low biomass in individual specimens (ca. 0.3 mg mean), which was insufficient to support the three different isotopic analyses (2.6 mg was needed). Since the foot contained the pedal ganglia and part of the digestive system, these structures were carefully removed from all specimens to avoid contamination and ensure foot tissue homogeneity. The shell length of the analysed specimens ranged from 8.1 mm to 12.8 mm, with no statistically significant differences among individuals from different sampling stations (one-way ANOVA: $F_{4,45} = 2.21$, $p = 0.083$; Table S3).

For the anemones, the body wall was dissected because it may be less prone to digestive contamination. Both internal and external sides of the body wall were carefully scraped with the non-cutting edge of a scalpel to prevent isotopic contamination from non-assimilated organic material and sediment resulting from the species' burrowing behaviour. As with bivalve specimens, medium-sized individuals (3.0–9.4 cm) were deliberately selected to minimise potential size-related variability in isotopic composition. However, no strict statistical procedure was applied to define the size range in this case, as the measured lengths are typically not representative of the specimens' actual living dimensions due to contraction upon collection.

The cleaned foot of each bivalve ($N = 50$) and a 1 cm^2 section of the body wall from each anemone ($N = 45$) were dried at 60 °C in an oven for 24 h and kept dry in a desiccator containing silica gel until encapsulation. For $\delta^{13}C$ and $\delta^{15}N$ analyses, 0.3 mg of tissue per sample was weighed, while $\delta^{34}S$ ones required 2 mg. Tin capsules of 3.3 × 5 mm (Lüdi Swiss; www.ludiswiss.com) were used for carbon and nitrogen measurements, and 5 × 8 mm capsules (Elemental Microanalysis; www.elementalmicroanalysis.com) were used for sulphur ones. A Mettler Toledo MX5 (www.mt.com) microbalance, with a sensitivity of 0.001 mg, was used for this purpose.

2.4. Stable isotope analysis

All tin capsules for $\delta^{13}C$ and $\delta^{15}N$ measurements were combusted at 900 °C and analysed using a continuous-flow isotope-ratio mass spectrometer (Delta V Advantage coupled to FLASH IRMS, Thermo Scientific; www.thermofisher.com) at the Centres Científics i Tecnològics of the Universitat de Barcelona (CCiT-UB). Their values were calibrated with a precision of ±0.3‰ using reference materials certified by the International Atomic Energy Agency (IAEA; www.iaea.org) in Vienna (Austria) and by the United States Geological Survey (USGS; www.usgs.gov), along with additional internal standards. For $\delta^{13}C$ measurements, these included polyethylene (IAEA-CH7, $\delta^{13}C = -32.15$‰), caffeine (IAEA-600, $\delta^{13}C = -27.77$‰; USGS62, $\delta^{13}C = -27.70$‰), animal hair (UCGEMA-P, $\delta^{13}C = -21.08$‰), shark collagen (UCGEMA-SC, $\delta^{13}C = -13.21$‰), and fructose ($\delta^{13}C = -10.80$‰). Similarly, $\delta^{15}N$ values were calibrated using ammonium sulphate (IAEA-N1, $\delta^{15}N = +0.43$‰), caffeine (IAEA-600, $\delta^{15}N = +1.00$‰; USGS62, $\delta^{15}N = +20.17$‰), potassium nitrate (USGS34, $\delta^{15}N = -1.80$‰), ammonium sulphate (USGS25, $\delta^{15}N = -30.41$‰), animal hair (UCGEMA-P, $\delta^{15}N = +7.60$‰), and shark collagen (UCGEMA-SC, $\delta^{15}N = +12.40$‰). All standards were used at the analyses' beginning and end, and one of them was also included after every 12 to 16 samples to recalibrate the system and correct for instrumental drift. Acetanilide was added to each standard run to control for elemental composition, enabling accurate calculation of the molar C:N ratio.

Regarding the $\delta^{34}S$ measurements, tin capsules were combusted at 1030 °C and analysed using another continuous-flow isotope-ratio mass spectrometer (Carlo Erba 1108 coupled to IRMS Delta Plus XP, Thermo Finnigan; www.thermofisher.com), also at the CCiT-UB. $\delta^{34}S$ calibration, with a precision of ±0.1‰, was based on an in-house barium sulphate standard (YCEM, $\delta^{34}S = +12.8$‰), along with certified reference materials by IAEA: silver sulphide (IAEA-S2, $\delta^{34}S = +22.7$‰) and barium sulphate (IAEA-SO-5, $\delta^{34}S = +0.5$‰; IAEA-SO-6, $\delta^{34}S = -34.1$‰). Vanadium pentoxide (V_2O_5) was added to each sample to ensure the complete oxidation of sulphur compounds during combustion. It acts as a catalytic oxidising agent that facilitates the quantitative conversion of sulphur to sulphur dioxide for isotopic analysis. In this case, all standards were used after every 12 samples.

Raw isotopic values were corrected using linear regression models based on reference materials with known isotopic compositions (Skrzypek, 2013), allowing normalisation to international reference scales. Stable isotope abundances are expressed in δ notation (‰), representing the relative difference in isotope ratios between a sample and a standard (Vienna Pee Dee Belemnite for carbon; atmospheric N_2 for nitrogen; and Vienna Canyon Diablo Troilite for sulphur), as follows:

$$\delta^{j}X\ (‰) = \left[\frac{\left({}^{j}X/{}^{i}X\right)_{sample}}{\left({}^{j}X/{}^{i}X\right)_{standard}} - 1\right] \times 1000$$

where ${}^{j}X$ is the heavier isotope and ${}^{i}X$ is the lighter one in both the sample and the international reference standard (Bond and Hobson, 2012).

Because lipids are depleted in ^{13}C compared to proteins and carbohydrates, high lipid content can heterogeneously bias bulk $\delta^{13}C$ values towards lower values (Bas and Cardona, 2018). Most C:N ratios in samples of both species exceeded the 3.5 threshold, which is considered indicative of substantial lipid content in tissues (Post et al., 2007). Therefore, the mathematical correction for aquatic organisms proposed by Post et al. (2007) was applied to all our $\delta^{13}C$ data to estimate the lipid-normalised $\delta^{13}C$ value for each sample on the basis of its C:N ratio, according to the following equation:

$$\delta^{13}C_{normalised} = \delta^{13}C_{untreated} - 3.32 + 0.99 \times C:N$$

Specimens were stored in ethanol before stable isotope analysis, so possible preservation effects were considered. Ethanol storage has been reported to have negligible effects on $\delta^{15}N$ and $\delta^{34}S$ values of animal tissues, although it may occasionally slightly increase $\delta^{13}C$ values (Javornik et al., 2019; Le Bourg et al., 2019). Given the small magnitude of this potential offset, no correction for ethanol preservation was applied. Nevertheless, $\delta^{13}C$ comparisons with literature values should be interpreted with caution.

2.5. Data analysis

All statistical analyses were conducted using the free software package R (v4.5.1; R Core Team, 2025) with a significance level of $\alpha = 0.05$ (Zar, 2010). No values were excluded from the analyses, as our dataset did not contain implausible measurements and we had no evidence of analytical errors.

To assess trends along the distance-to-glacier gradient, linear models were fitted separately for each fjord and species, using biological measurements ($\delta^{13}C$, $\delta^{15}N$, $\delta^{34}S$, and C:N ratios) as response variables, and distance from the current glacier terminus as a continuous fixed effect. The number of years since ice cover was excluded because it was collinear with distance from the glaciers, which better represents environmental gradients and thus aligns more closely with our objective regarding overall fjord trends. Shapiro-Wilk tests (Shapiro and Wilk, 1965) and quantile-quantile (Q-Q) plots on residuals were used to test normality. Linearity was assessed using component-plus-residual plots (Fox, 1991), the inclusion of quadratic terms, and comparisons with generalised additive models. To evaluate potential intra-group

dependence, we calculated intraclass correlation coefficients (Shrout and Fleiss, 1979; Nakagawa and Schielzeth, 2010) and performed likelihood ratio tests (LRT; Self and Liang, 1987) comparing models with and without random intercepts. When these tests indicated significant dependence, we fitted linear mixed-effects (LME) models with random intercepts for sampling station (Laird and Ware, 1982; Pinheiro and Bates, 2000). Homoscedasticity was evaluated using the Breusch-Pagan test (Breusch and Pagan, 1979) and visual inspection of residuals (Zuur et al., 2009). When heteroscedasticity across stations was detected, generalised least squares (GLS) were used, or variance structures were incorporated into LME models. Model selection was based on the corrected Akaike's Information Criterion (AICc; Burnham and Anderson, 2004), selecting the one with the lowest AICc values (Zuur et al., 2009). This protocol was also followed for the examination of pairwise relationships among stable isotope and C:N ratios. For basic linear regressions, the coefficient of determination (R^2) was calculated to assess model fit (Zar, 2010). The analyses were conducted with the packages *nlme* (Pinheiro and Bates, 2025), *lmerTest* (Kuznetsova et al., 2020), *mgcv* (Wood, 2025), *performance* (Lüdecke et al., 2025), *car* (Fox et al., 2024), and *lmtest* (Hothorn et al., 2022).

For all response variables, except $\delta^{13}C$ in the bivalve, the models did not yield statistically significant distance effects. Thus, we further explored potential local spatial differences among stations using a categorical approach. These analyses were conducted separately for each fjord and species, using the sampling station as the categorical factor (e.g., MC1–MC5) and biological variables (i.e., $\delta^{13}C$, $\delta^{15}N$, $\delta^{34}S$, and C:N ratios) as response factors. Specifically, one-way ANOVA was conducted when the assumptions of normality and homogeneity of variances were met (Zuur et al., 2010). In this case, homogeneity of variances among stations was tested using Levene's test (Gastwirth et al., 2009) and the residuals-versus-fitted-values plot (Zuur et al., 2009). When heteroscedasticity was detected, Welch's ANOVA was applied instead, as it adjusts the F-test to account for differences in group variances (Welch, 1951). Post-hoc pairwise comparisons were conducted to evaluate differences between groups, using Tukey's Honest Significant Difference (HSD) test (Tukey, 1949), or the Games-Howell test for heteroscedastic data (Games and Howell, 1976). These post-hoc comparisons also assessed the local influence of seabed morphology on the ecology and nutritional condition of the study species. The environmental data (fluorescence and dissolved oxygen) were also analysed using this approach, considering the sampling station as a categorical factor and each environmental variable as a response factor. Additionally, the effect of depth on $\delta^{15}N$ was evaluated separately for each species within each fjord using linear models, but no significant results were found. All these analyses were performed using the *rstatix* package (Kassambara, 2025). No statistical comparisons were performed between fjords or between species at any stage of the analyses.

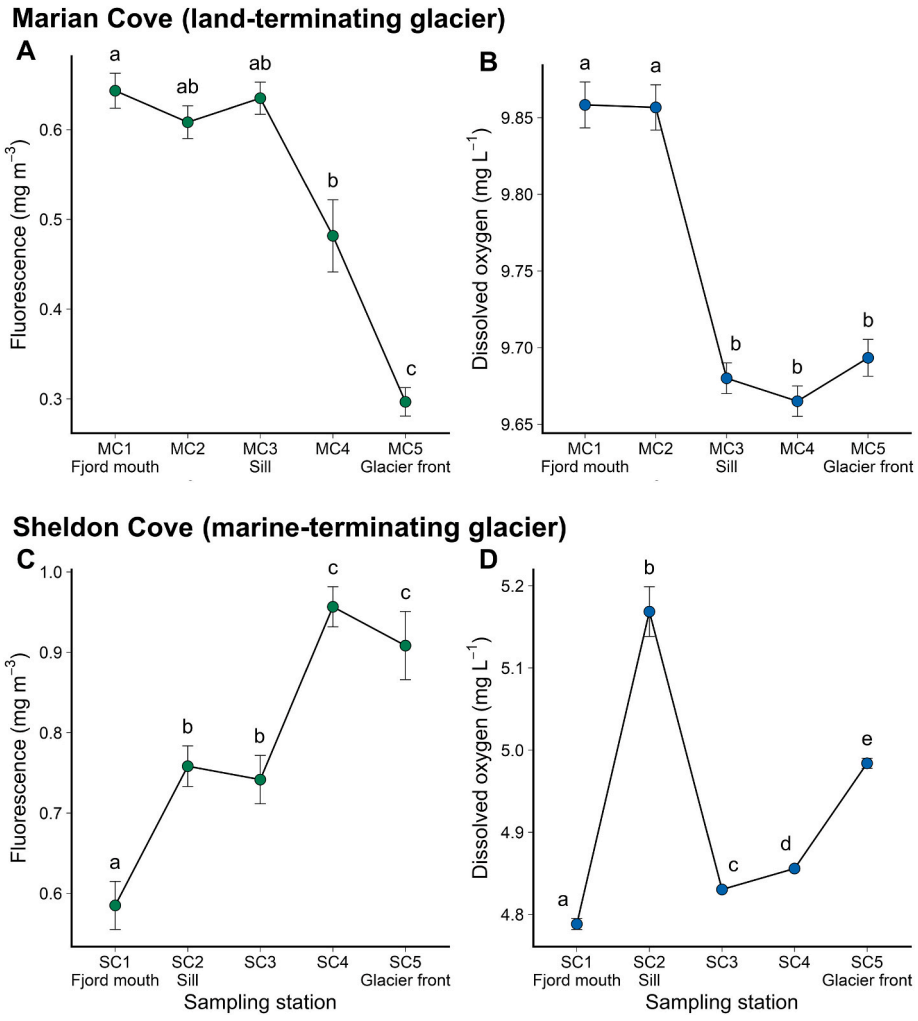

Fig. 2. Fluorescence and dissolved oxygen across Marian Cove and Sheldon Cove (WAP). Mean (±SE) values showing spatial variation in fluorescence (mg m^{-3}; A) and dissolved oxygen (mg L^{-1}; B) in Marian Cove, and fluorescence (C) and dissolved oxygen (D) in Sheldon Cove. Sampling stations ($n = 6$ per station) are ordered from the fjord mouth on the left (MC1/SC1) towards the glacier edge on the right (MC5/SC5), with the location of the submarine sills indicated (MC3/SC2). Different letters denote significant differences among stations. Y-axis scales differ among panels to allow clearer visualisation of spatial variation within each fjord.

3. Results

3.1. Fluorescence and dissolved oxygen variation within each fjord

In the land-terminating glacier regime of Marian Cove, fluorescence and dissolved oxygen both differed across stations ($p < 0.001$; Fig. 2A and B; Table S4), increasing away from the glacier. For example, fluorescence was significantly lower at the innermost station (MC5) than at all other stations. Dissolved oxygen showed lower concentrations at the inner stations (MC3–MC5) than at the outer stations (MC1–MC2).

Within the marine-terminating glacier regime of Sheldon Cove, fluorescence varied significantly as well ($p < 0.001$; Fig. 2C; Table S4), but in the opposite direction to that in Marian Cove. Values increased from the outermost to the innermost stations, indicating a progressive increase in fluorescence from the fjord mouth. Oxygen concentrations also differed markedly across stations ($p < 0.001$; Fig. 2D), reaching a maximum at the sill and being relatively elevated towards the glacier front.

3.2. Stable isotope and C:N ratios variation within each fjord

In Marian Cove, $\delta^{13}C$ values in the bivalve (−21.24‰ to −18.70‰; Table 1) increased significantly with distance from the glacier ($\beta = 0.145\ km^{-1}$, $p = 0.001$; Fig. S1), as indicated by a GLS model. This means that $\delta^{13}C$ values progressively decreased towards the closest station to the glacier terminus. Despite overall variability being modest, station-wise differences were also significant ($p = 0.025$; Fig. 3A; Table S5), with MC3 being ^{13}C-depleted compared to the outermost station (MC1). $\delta^{15}N$ (6.29‰ to 9.68‰; Table 1) also varied across stations ($p < 0.001$; Fig. 3B), without a clear pattern along the gradient. There were lower $\delta^{15}N$ values at MC5 compared to MC1 and MC3 (sill), and higher values at the sill than at MC2. The mean at the sill was marginally higher than the heterogeneous MC4 ($p = 0.062$). $\delta^{34}S$ values spanned a wide range (3.61‰ to 14.79‰; Table 1) and station-wise differences were also significant ($p < 0.001$; Fig. 3C), as bivalves at the sill and at MC5 were ^{34}S-enriched compared to MC2. Finally, C:N ratios (3.41 to 4.29; Table 1) differed significantly among stations as well ($p = 0.002$; Fig. 3D), with higher values at the sill than at MC2 or MC4.

In Sheldon Cove, $\delta^{13}C$ values in the sea anemone (−20.33‰ to −17.30‰; Table 1) varied markedly among stations ($p < 0.001$; Fig. 4A; Table S6), with higher values near the glacier front. Individuals at the innermost station (SC5) were significantly ^{13}C-enriched compared to all other stations. SC2 (sill) showed higher $\delta^{13}C$ values compared to SC3 and SC4. $\delta^{15}N$ values (9.00‰ to 12.85‰; Table 1) also showed spatial structuring ($p < 0.001$; Fig. 4B). Enrichment in ^{15}N occurred at the sill relative to SC3, SC4, and SC5, while SC4 values were lower than SC1. $\delta^{34}S$ ranged from 12.72‰ to 20.30‰ (Table 1) and differed across stations as well ($p = 0.025$; Fig. 4C), with ^{34}S enrichment at SC5 relative to SC3. Finally, C:N ratios (3.56 to 4.54; Table 1) showed no significant spatial variation ($p = 0.755$; Fig. 4D).

3.3. Bivariate relationships among biological variables in each species

In the bivalve, $\delta^{34}S$ decreased with $\delta^{13}C$ and showed a significant concave-down quadratic relationship ($\beta_1 = -1.673$, $p_1 < 0.001$; $\beta_2 = -0.637$, $p_2 = 0.002$; Fig. 5A). Additionally, $\delta^{15}N$ increased with $\delta^{34}S$ (LME: $\beta = 0.192$, $p < 0.001$). C:N ratios were positively associated with both $\delta^{15}N$ ($\beta = 0.083$, $p < 0.001$, $R^2 = 0.22$) and $\delta^{34}S$ (GLS: $\beta = 0.031$, $p < 0.001$; Fig. 5B). In the anemone, $\delta^{15}N$ increased with $\delta^{13}C$ (GLS: $\beta = 0.220$, $p = 0.005$). $\delta^{34}S$ increased both with $\delta^{13}C$ ($\beta = 0.777$, $p = 0.013$, $R^2 = 0.13$; Fig. 5C) and C:N ratios ($\beta = 0.046$, $p = 0.010$, $R^2 = 0.13$; Fig. 5D). No other significant relationships among biological variables were detected in either species.

4. Discussion

Antarctic fjords show strong gradients in biota–environment interactions (e.g., see Zwerschke et al., 2022; Simmons et al., 2025). Here, we provide new evidence of stable isotope and C:N ratio variation in shallow-shelf soft-bottom invertebrates within Antarctic glacier-influenced fjords. In Marian Cove, the decreasing pattern in $\delta^{13}C$ that we found in the bivalve *Nuculana inaequisculpta* towards the glacier terminus may reflect environmental conditions associated with surface meltwater discharge. Such run-off from a land-terminating glacier could reduce primary production near the glacier front (Kim et al., 2021). In Sheldon Cove, the sea anemone *Edwardsia* sp. displayed the highest $\delta^{13}C$ values near the glacier terminus. This trend may be linked to subsurface meltwater input from the marine-terminating glacier, which could promote phytoplankton growth in the inner fjord (Jones et al., 2023). Thus, glacier configuration may indirectly shape isotopic responses by influencing where meltwater enters the fjord and where primary production is enhanced. By contrast, $\delta^{15}N$, $\delta^{34}S$, and C:N ratios appear to be driven by the feeding strategy and local conditions such as seabed morphology.

4.1. Stable isotope comparison in an Antarctic context

Station MC4 served as our reference in Marian Cove, as it lies far from direct bloom and sill influence and is not adjacent to the glacier. There, *Nuculana inaequisculpta* exhibited intermediate $\delta^{13}C$ and C:N ratios compared with previous data of Antarctic bivalves (Dunton, 2001; Corbisier et al., 2004; Mincks et al., 2008, Table 2). Its $\delta^{15}N$ values were similar to those of the protobranch *Aequiyoldia eightsii* (Corbisier et al., 2010; Pasotti et al., 2015b), and both were higher than those typically reported for Antarctic non-protobranch bivalves (Mincks et al., 2008; Michel et al., 2019; Alurralde et al., 2020). This likely reflects the deposit-feeding strategy of protobranchs, as sedimentary organic matter has undergone microbial processing, resulting in higher $\delta^{15}N$ values than those of the fresh phytoplankton used by suspension-feeding bivalves (Iken et al., 2001). An elevated $\delta^{15}N$ baseline in Marian Cove (discussed below) may have also contributed to the observed mean. $\delta^{34}S$ values of *N. inaequisculpta* were lower than those reported in the only

Table 1
Mean (±SD) stable isotope and C:N ratios from each of the five sampling stations ($n = 10$) along Marian Cove (MC) and Sheldon Cove (SC), WAP. MC1/SC1 = outermost; MC5/SC5 = innermost.

Species	Station	$\delta^{13}C$ (‰)	$\delta^{15}N$ (‰)	$\delta^{34}S$ (‰)	C:N ratio
Nuculana inaequisculpta	**MC1**	−19.59 ± 0.30	8.35 ± 1.05	9.36 ± 3.53	3.90 ± 0.20
	MC2	−19.84 ± 0.18	7.52 ± 0.57	5.78 ± 0.40	3.74 ± 0.06
	MC3	−20.02 ± 0.23	8.94 ± 0.67	10.84 ± 1.54	4.02 ± 0.15
	MC4	−19.87 ± 0.68	7.94 ± 1.02	9.33 ± 4.29	3.80 ± 0.18
	MC5	−20.13 ± 0.65	7.28 ± 0.64	9.96 ± 0.96	3.84 ± 0.12
***Edwardsia* sp.**	**SC1**	−19.47 ± 0.55	11.06 ± 0.66	16.38 ± 2.92	4.07 ± 0.30
	SC2	−19.34 ± 0.40	11.72 ± 1.03	17.38 ± 0.69	4.03 ± 0.22
	SC3	−20.00 ± 0.29	10.07 ± 0.60	15.29 ± 1.39	4.01 ± 0.16
	SC4	−19.92 ± 0.23	9.97 ± 0.61	17.20 ± 1.89	4.11 ± 0.15
	SC5	−18.00 ± 0.49	10.60 ± 0.28	17.52 ± 1.52	3.99 ± 0.28

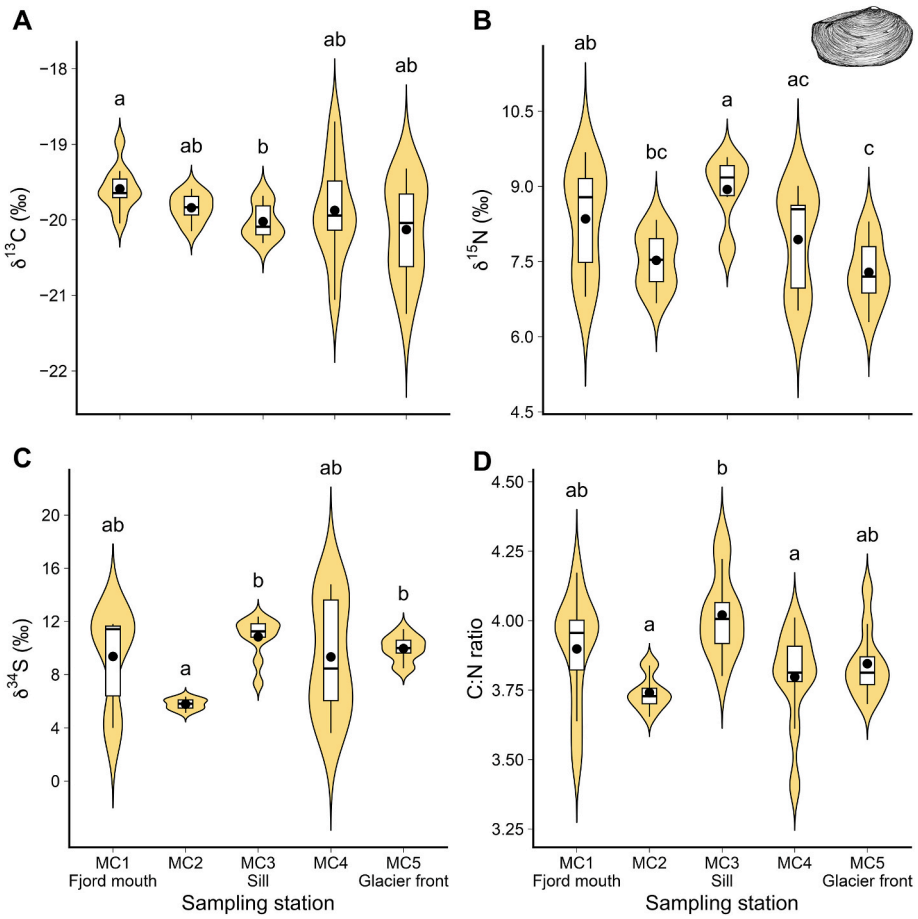

Fig. 3. Stable isotope and C:N ratios of the bivalve *Nuculana inaequisculpta* across the land-terminating glacier of Marian Cove (WAP). Violin plots with embedded boxplots and means (points) show spatial variation in $\delta^{13}C$ (A), $\delta^{15}N$ (B), $\delta^{34}S$ (C), and C:N ratios (D) across five sampling stations ($n = 10$). These stations were arranged along a glacier-influence gradient, from MC1 (furthest from the glacier) on the left to MC5 (closest to the glacier) on the right, including MC3 (near a submarine sill). Different letters indicate significant differences among stations. * For $\delta^{13}C$, a GLS model revealed a significant positive relationship with distance from the glacier front ($\beta = 0.145$, $p = 0.001$).

other $\delta^{34}S$ study available for Antarctic non-protobranch bivalves (Michel et al., 2019). The low $\delta^{34}S$ observed is consistent with its deposit-feeding habit and the contribution of suboxic sedimentary sources (see below).

The outermost station of Sheldon Cove served as our reference for *Edwardsia* sp., being far from direct bloom, sill and glacier influence. There, its $\delta^{13}C$ and C:N ratios fell within the variability reported for other Antarctic anthozoans (Dunton, 2001; Mincks et al., 2008; Gillies et al., 2012, Table 3). *Edwardsia* sp. exhibited relatively high $\delta^{15}N$ values (Mincks et al., 2008; Gillies et al., 2013), which may be linked to the high nitrogen baseline expected in glacier-influenced fjords (see below). To the best of our knowledge, this study provides the second $\delta^{34}S$ record for Antarctic anthozoans, the previous one being lower (Michel et al., 2019). These relatively low $\delta^{34}S$ values are consistent with sulphur sources linked to the water column (Silva and Vargas, 2014; Björk et al., 2017). *Edwardsia* sp. typically feeds on material derived from the water column, where the sulphur pool is more oxidised and enriched in ^{34}S (Daly et al., 2012; Szpak and Buckley, 2020).

4.2. Ecological trends across glacier-influence gradients

In Marian Cove, the lower fluorescence observed near the glacier front and the increasing trend toward the outer stations are consistent with the physical and biogeochemical characteristics of a land-terminating glacier system. Here, meltwater is discharged directly at the surface, producing a highly turbid plume that stratifies the water column, limits light penetration, and dilutes surface nutrient concentrations, thereby constraining phytoplankton growth near the glacier (Holding et al., 2019; Kim et al., 2021; Demidov et al., 2023; Jones et al., 2023; Hoshiba et al., 2024). In Sheldon Cove, fluorescence was highest near the glacier, where meltwater inflow occurs at depth rather than at the surface. This deep input entrains nutrient-rich waters upward, alleviating nutrient limitation and stimulating phytoplankton growth near the glacier front (Jones et al., 2023).

Data from such research cruises provide only a limited snapshot of fluorescence, whereas the isotopic signal in the study species offers a more reliable, time-integrated record, since their tissues' turnover may occur over weeks to months (Vander Zanden et al., 2015). Within each fjord, $\delta^{13}C$ variation aligned with the local productivity pattern observed along the transect. In Marian Cove, the bivalve exhibited an increase in $\delta^{13}C$ values toward the fjord mouth, where the fluorescence was maximum. Lee et al. (2025) also worked in Marian Cove but reported a ^{13}C enrichment near the glacier based on intertidal samples, possibly reflecting depth-related differences in food availability. In Sheldon Cove, the sea anemone showed the highest $\delta^{13}C$ values at the innermost site, adjacent to the glacier front. This also aligns with the higher fluorescence concentrations near the glacier edge. Therefore, these high $\delta^{13}C$ values were likely driven by the strong phytoplankton blooms. Rapid CO_2 uptake can cause ^{13}C local depletion, driving phytoplankton to use bicarbonate (HCO_3^-) instead, which is ^{13}C-enriched (Rau et al., 1989). This shift raises $\delta^{13}C$ values in primary producers and, consequently, in benthic consumers (Bae et al., 2021; Lee

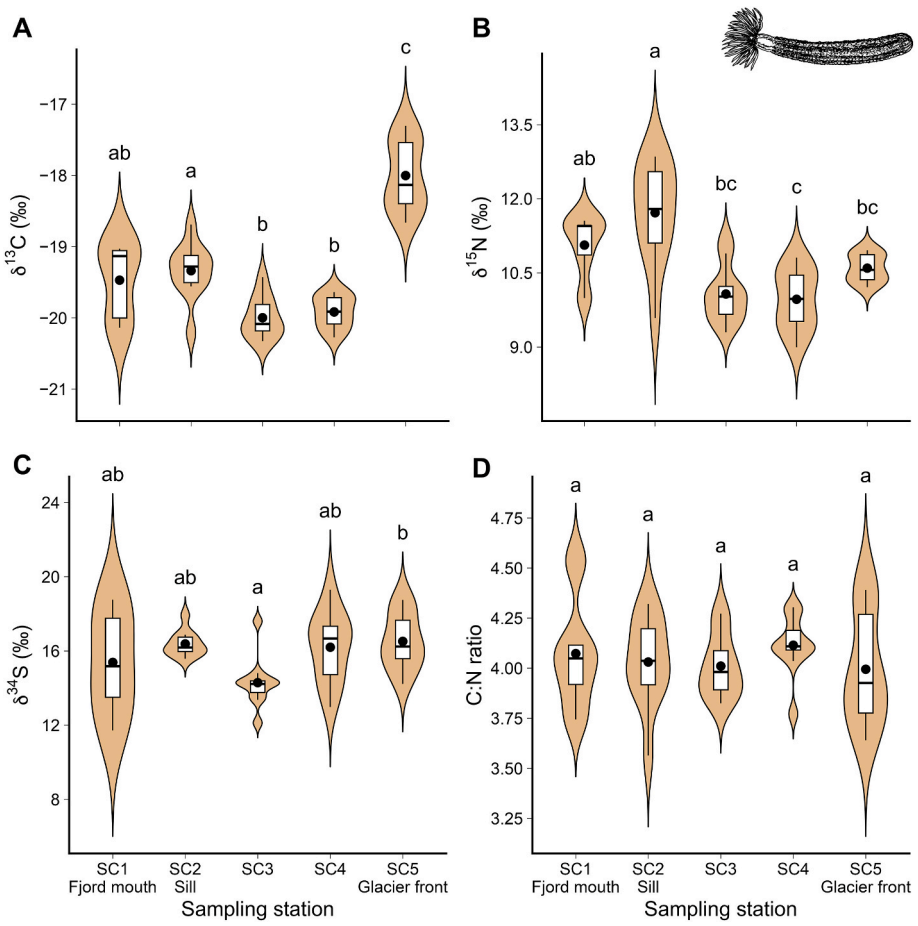

Fig. 4. Stable isotope and C:N ratios of the sea anemone *Edwardsia* sp. across the marine-terminating glacier of Sheldon Cove (WAP). Violin plots with embedded boxplots and means (points) show spatial variation in $\delta^{13}C$ (A), $\delta^{15}N$ (B), $\delta^{34}S$ (C), and C:N ratios (D) across five sampling stations ($n = 10$). These stations were arranged along a glacier-influence gradient, from SC1 (furthest from the glacier) on the left to SC5 (closest to the glacier) on the right, including SC2 (near a submarine sill). Different letters indicate significant differences among stations.

et al., 2025).

The low $\delta^{13}C$ values near the glacier front in our studied bivalve species from Marian Cove are contrary to the pattern found so far in Antarctic fjords (Alurralde et al., 2020; Jędruch et al., 2025; Lee et al., 2025). Reduced primary productivity driven by sediment-laden runoff from melting land-terminating glaciers along the WAP may counteract the negative climate feedback associated with the formation of new ice-free habitats (Alurralde et al., 2019). Together, our results suggest that the environmental setting associated with the glacier configuration may influence the spatial patterns of phytoplankton biomass and, consequently, the carbon sources supporting benthic food webs within each fjord. Spatial $\delta^{13}C$ variability in benthic fauna within glacier-influenced fjords is here suggested to result from phytoplankton primary production rather than solely from a spatial gradient linked to glacier proximity.

Bottom-water dissolved oxygen provides additional context for interpreting the benthic isotopic signals. In Marian Cove, lower oxygen values near the land-terminating glacier are consistent with a more stratified, meltwater-influenced environment, where surface freshwater input limits vertical exchange (Kim et al., 2021; Jones et al., 2023). In Sheldon Cove, bottom-water dissolved oxygen was relatively elevated towards the marine-terminating glacier, likely because subsurface meltwater discharge drives buoyant plume circulation near the glacier face (Straneo and Cenedese, 2015; Jones et al., 2023) and active phytoplankton blooms supply oxygen to surface waters.

The lack of a consistent pattern in the nitrogen stable isotope ratio with distance from the glaciers aligns with previous findings (Alurralde et al., 2020; Lee et al., 2025). Jędruch et al. (2025) documented higher $\delta^{15}N$ values from glacier-adjacent stations, but attributed the enrichment to the influence of nearby penguin rookeries in Admiralty Bay (King George Island, South Shetland Islands, WAP). Trophic levels may have varied due to local factors such as the presence of submarine sills, as we discuss later. There was also no consistent trend in $\delta^{34}S$ values along the distance gradients from the glacier edges, which is also in agreement with previous reports (Jędruch et al., 2025). In fjords, suboxic conditions are pervasive throughout the sedimentary environment (Silva and Vargas, 2014; Björk et al., 2017). Moreover, $\delta^{34}S$ values could have been influenced by individuals' reliance on sedimentary food sources. Consequently, a spatially heterogeneous pattern emerges, driven by local and individual variations in these factors. Similarly, no clear trends were detected in C:N ratios (Jędruch et al., 2025), as the nutritional condition was partially constrained by the reliance on feeding sources from the suboxic sediment (see below).

4.3. Patterns of $\delta^{15}N$ and $\delta^{34}S$ for trophic complexity and environmental features

Before interpreting $\delta^{15}N$ variability as evidence of trophic differences, it is important to consider that $\delta^{15}N$ values may also reflect variation in the isotopic baseline. The $\delta^{15}N$ composition of phytoplankton-derived food sources can vary according to the nitrogen source assimilated by phytoplankton, because nitrate and ammonium uptake involve different isotope effects (Waser et al., 1998). This is particularly relevant in Southern Ocean systems, where phytoplankton

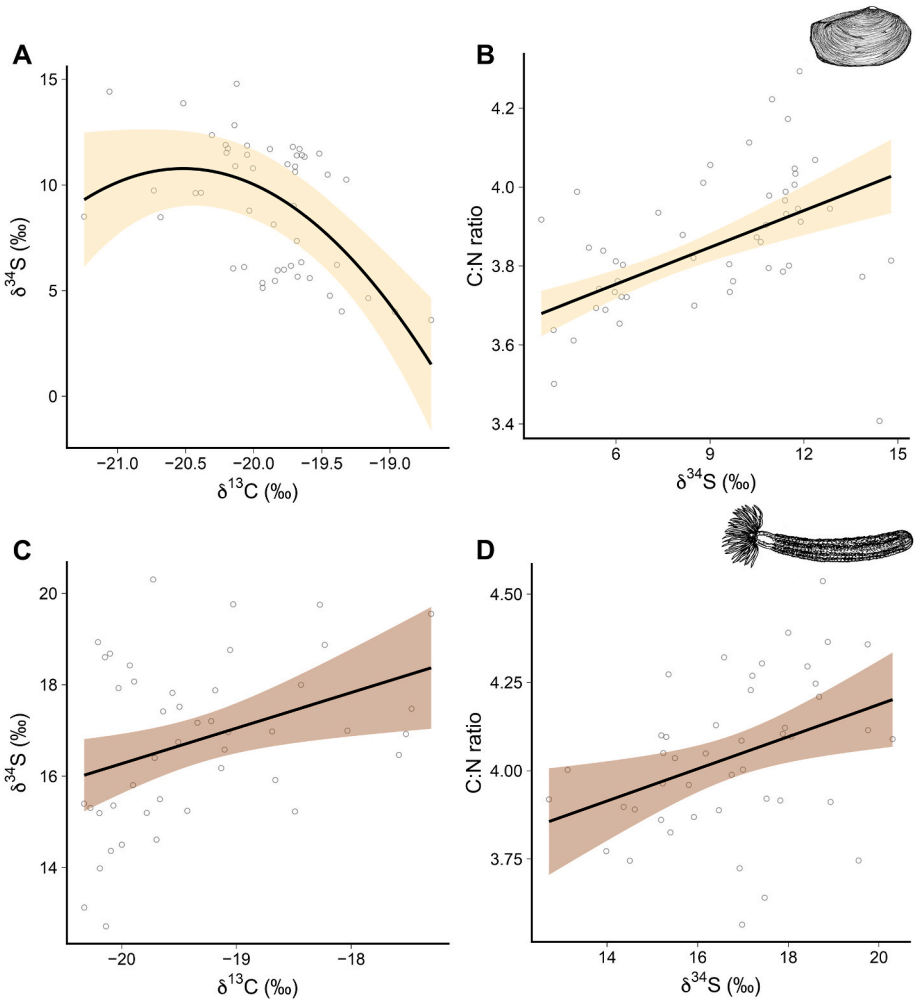

Fig. 5. Stable isotope and C:N ratio relationships in the study species. Quadratic relationship between $\delta^{34}S$ and $\delta^{13}C$ (A) and linear relationship between C:N ratio and $\delta^{34}S$ (B) in the bivalve *Nuculana inaequisculpta* from the land-terminating glacier of Marian Cove ($N = 50$). Linear relationship between $\delta^{34}S$ and $\delta^{13}C$ (C) and between C:N ratio and $\delta^{34}S$ (D) in the sea anemone *Edwardsia* sp. from the marine-terminating glacier of Sheldon Cove ($N = 45$). Each point represents an individual. Black lines indicate model fits and shaded areas denote 95% confidence intervals.

Table 2
Mean stable isotope and C:N ratios reported in Antarctic bivalve species. EA: East Antarctica; KGI: King George Island; WAP: Western Antarctic Peninsula.

Species	Location	$\delta^{13}C$ (‰)	$\delta^{15}N$ (‰)	$\delta^{34}S$ (‰)	C:N ratio	Reference
Aequiyoldia eightsii (Protobranchia)	KGI, WAP	−10.0	7.0			Corbisier et al. (2010)
	KGI, WAP	−12.3	7.5			Corbisier et al. (2010)
	KGI, WAP	−11.8 ± 0.8	8.8 ± 0.4			Pasotti et al. (2015b)
	KGI, WAP	−18.0 ± 2.9				Corbisier et al. (2004)
	Anvers Island, WAP	−17.5 ± 0.7	6.7 ± 0.2		4.6	Dunton (2001)
Nuculana inaequisculpta(Protobranchia)	KGI, WAP	−19.9 ± 0.7	7.9 ± 1.0	9.3 ± 4.3	3.8 ± 0.2	This study (MC4)
Adamussium colbecki	Adélie Land, EA	−19.5 ± 0.6	4.5 ± 0.3	14.6 ± 0.9		Michel et al. (2019)
	Princess Elizabeth Land, EA	−19.7 ± 0.2	6.8 ± 0.3			Gillies et al. (2013)
	Wilkes Land, EA	−17.7 ± 0.3	5.9 ± 0.2			Gillies et al. (2012)
Laternula elliptica	KGI, WAP	−23.9	2.7			Corbisier et al. (2010)
	KGI, WAP	−23.4	3.3			Corbisier et al. (2010)
	KGI, WAP	−23.0 ± 0.1	3.4 ± 0.4		4.1 ± 0.1	Alurralde et al. (2020)
	KGI, WAP	−26.7 ± 0.1				Corbisier et al. (2004)
	Anvers Island, WAP	−23.2 ± 0.8	5.7 ± 0.6		5.6 ± 0.4	Dunton (2001)
	Adélie Land, EA	−22.4 ± 1.5	4.4 ± 0.5	15.4 ± 0.6		Michel et al. (2019)
	Princess Elizabeth Land, EA	−19.7 ± 0.4	6.8 ± 0.3			Gillies et al. (2013)
	Wilkes Land, EA	−16.6 ± 0.2	6.4 ± 0.2			Gillies et al. (2012)
Limopsis marionensis	Anvers Island, WAP	−21.9 ± 0.1	10.1 ± 0.1		3.3 ± 0.0	Mincks et al. (2008)

nitrogen uptake can shift from nitrate-based to ammonium-based production and ammonium may become an important nitrogen source even when nitrate remains available (Goeyens et al., 1995). Such baseline differences may propagate through the food web, influencing $\delta^{15}N$ values in benthic consumers.

N. inaequisculpta showed substantial $\delta^{15}N$ variability both within

Table 3
Mean stable isotope and C:N ratios reported in Antarctic anthozoan species. EA: East Antarctica; KGI: King George Island; WAP: Western Antarctic Peninsula.

Species	Location	$\delta^{13}C$ (‰)	$\delta^{15}N$ (‰)	$\delta^{34}S$ (‰)	C:N ratio	Reference
Artemidactis victrix (Actiniaria)	Princess Elizabeth Land, EA	−16.0 ± 0.5	12.0 ± 0.7			Gillies et al. (2013)
Edwardsia sp. (Actiniaria)	KGI, WAP	−19.5 ± 0.6	11.1 ± 0.7	16.4 ± 2.9	4.1 ± 0.3	This study (outermost station)
Hormathia lacunifera(Actiniaria)	Anvers Island, WAP	−22.2 ± 0.2	8.9 ± 0.2		3.1 ± 0.3	Mincks et al. (2008)
Isosicyonis alba (Actiniaria)	Anvers Island, WAP	−26.5 ± 0.5	8.3 ± 0.4		4.5 ± 0.2	Mincks et al. (2008)
Isotealia antarctica (Actiniaria)	Princess Elizabeth Land, EA	−17.1	12.8			Gillies et al. (2013)
	Adélie Land, EA	−16.2 ± 1.2	10.7 ± 0.8	−11.8 ± 1.5		Michel et al. (2019)
Stomphia selaginella (Actiniaria)	Princess Elizabeth Land, EA	−17.2 ± 1.0	11.6 ± 0.9			Gillies et al. (2013)
Urticinopsis antarctica (Actiniaria)	Princess Elizabeth Land, EA	−15.6 ± 1.4	11.5 ± 1.0			Gillies et al. (2013)
	Wilkes Land, EA	−15.1 ± 0.4	10.6 ± 0.1			Gillies et al. (2012)
Not specified (Actiniaria)	KGI, WAP	−26.5				Corbisier et al. (2004)
Anthomastus bathyproctus	KGI, WAP	−23.8 ± 0.6	4.2 ± 0.3			Elias-Piera (2015)
Malacobelemnon daytoni	KGI, WAP	−22.6 ± 0.3	7.1 ± 0.2			Pasotti et al. (2015b)
	KGI, WAP	−25.0 ± 0.3	6.9 ± 0.2		4.3 ± 0.0	Alurralde et al. (2020)
Pennatulacea sp.	Princess Elizabeth Land, EA	−20.8 ± 0.4	8.8 ± 0.6			Gillies et al. (2013)
Primnoisis sp.	KGI, WAP	−17.9	9.5			Elias-Piera (2015)
Not specified	Bransfield Strait	−26.3	5.8			Elias-Piera (2015)
	Anvers Island, WAP	−24.5 ± 0.3	6.0 ± 0.1		5.8	Dunton (2001)

stations and along the Marian Cove transect. Although variability in the $\delta^{15}N$ values of *N. inaequisculpta* might result from differences in baseline, the heterogeneity reported here within the same population suggests the presence of two distinct trophic strategies. Although most protobranchs have been traditionally considered deposit feeders, Zardus (2002) proposed that specialised gill function in nuculanaceans may enable a greater reliance on filter feeding compared to other protobranchs. This hypothesis is further supported by the high $\delta^{34}S$ variability observed within Marian Cove stations, as the filter-feeding strategy of some individuals would facilitate the incorporation of sulphur from the water column, thereby avoiding sedimentary sources in fjord suboxic conditions. *A. eightsii* is another protobranch known for its flexible feeding strategy, typically using deposit feeding but facultatively switching to filter feeding when phytoplankton becomes more available in the water column (Davenport, 1988). *N. inaequisculpta* may also adopt a flexible strategy, depending on local food availability, that involves both deposit and filter feeding. That versatility could be ecologically advantageous in Antarctic glacier-influenced environments, where sedimentation and phytoplankton inputs are pivotal biological drivers (Alderkamp et al., 2012).

In the studied fjord environments, $\delta^{34}S$ values were markedly lower than the typical marine sulphate signature (ca. 21‰; Markovic et al., 2015). This suggests sediment-intense dissimilatory sulphate reduction and suboxic conditions (Fry et al., 1986; Raoult et al., 2024). There, the accumulation of glacially derived and other fjord sediments, along with phytoplanktonic debris, could increase oxygen demand (Silva and Vargas, 2014; Björk et al., 2017). Together with the deep depths, strong stratification, low bioturbation, and the restricted water exchange typical of semi-enclosed environments, these conditions may contribute to suboxia in both fjords (Silva and Vargas, 2014; Björk et al., 2017). Their seabed is thus consistent with the activity of sulphate-reducing bacteria (SRB), which typically inhabit suboxic to anoxic and organically enriched sediments (Muyzer and Stams, 2008). These SRB preferentially reduce ^{32}S and their anaerobic respiration results in the production of ^{34}S-depleted hydrogen sulphide (H_2S; Canfield, 2001). Importantly, bottom-water dissolved oxygen reflects water-column ventilation and does not necessarily indicate the redox state of the underlying sediments, where oxygen demand from organic matter degradation can produce suboxic conditions even beneath well-oxygenated water.

Suboxic conditions at the bottom of the water column and in the sediments may have contributed to elevated baseline $\delta^{15}N$ values in these glacier-influenced fjords. High $\delta^{15}N$ baselines are typically associated with intense nitrogen recycling processes (Hoefs, 2021; Fraser et al., 2024). Here, the sedimentary accumulation of H_2S and low oxygen conditions favour denitrifying bacteria (Pratihary et al., 2023). Denitrification preferentially removes the lighter nitrogen isotope (^{14}N), leading to the accumulation of ^{15}N in the remaining nitrate pool (Altabet, 2007). Although denitrification occurs under suboxic conditions in the water column and the benthos, vertical mixing redistributes the enriched nitrate throughout the system. Consequently, new superficial primary producers incorporate nitrate that is already enriched in ^{15}N, increasing nitrogen stable isotope ratios at the base of the food web. This mechanism is consistent with previous findings, as phytoplankton ^{15}N values in glacier-influenced fjords (ca. 6‰; Lee et al., 2025) are notably higher than those in non-glacial areas such as Fildes Bay (King George Island; ca. 2‰; Cardona et al., 2021).

4.4. Individual-level relationships between biological variables

$\delta^{13}C$–$\delta^{34}S$ relationships at the individual level provided additional insights into how different glacier-driven changes in primary production may affect benthic organisms. In the bivalve, the concave-down $\delta^{13}C$–$\delta^{34}S$ trend suggests higher sedimentary suboxia at stations closest to the influence of the phytoplankton bloom. The observed pattern likely indicates that only strong phytoplankton blooms are sufficient to change the sediment suboxic conditions. Moderate phytoplankton inputs may lead to ^{13}C enrichment without strongly affecting sulphur cycling, but intense blooms can deplete oxygen, stimulate SRB activity, and yield isotopically lighter sulphur in deposit feeders (Canfield, 2001).

In the anemone, the positive $\delta^{13}C$–$\delta^{34}S$ relationship suggests reduced reliance on suboxic sedimentary food and greater use of water-column prey near glacier blooms. Thus, anemones may benefit from bloom-driven food pulses by directly capturing pelagic material, avoiding suboxic sediments (Daly et al., 2012). Such flexibility highlights their ability as suspension feeders to exploit transient pelagic inputs generated by glacier-driven blooms. These results suggest that resilience to climate-driven changes in fjord productivity and oxygen dynamics may depend, at least in part, on the main feeding strategy of each benthic species. This interpretation is further reinforced by the positive $\delta^{13}C$–$\delta^{15}N$ relationship found in the anemone, indicating that individuals feeding near the bloom also occupy higher trophic positions.

Moreover, the positive relationship between $\delta^{34}S$ and C:N ratios at the individual level in both taxa suggests that higher carbon content was associated with a lower reliance on sediment organic matter and a greater contribution from water-column sources. Beyond sediment suboxia coupled with oxygen consumption by SRB, an additional mechanism explaining this strong linkage may involve competition for organic matter between SRB and benthic invertebrates when they feed on sediment. SRB also produce sulphide, a compound highly toxic to animals (Levin et al., 2009; Vaquer-Sunyer and Duarte, 2010). In

parallel, for the bivalve, $\delta^{15}N$ is positively related to both $\delta^{34}S$ and C:N ratios, indicating that lower sediment reliance and higher nutritional condition is associated with a higher trophic level.

4.5. Influence of seabed morphology on ecology and nutritional condition

Spatial variability in $\delta^{15}N$, $\delta^{34}S$, and C:N ratios appears to be primarily driven by local habitat conditions, with seabed morphology as one possible factor. Bathymetric surveys revealed prominent underwater sills within the fjord transects in both Marian Cove and Sheldon Cove (Sands et al., 2018), located at 107 m and 175 m depth, respectively. In the case of the bivalve, the sill-associated station in Marian Cove (MC3) exhibited higher C:N ratios compared to both adjacent stations. In addition, $\delta^{15}N$ and $\delta^{34}S$ values were higher than in one neighbouring station, although not relative to the other, where these isotopic variables were highly heterogeneous (in the case of $\delta^{15}N$, there was a marginal difference). The $\delta^{34}S$ pattern suggests that the sill enhances water renewal and, therefore, promotes the filter-feeding strategy in the bivalve. The elevated $\delta^{15}N$ values further indicate that bivalve individuals at this location might be exploiting prey at a higher trophic level. Those differences are unlikely to result from differences in the baseline, since all the stations are below the photic zone and therefore do not integrate primary production generated locally at the benthic sampling sites. Moreover, Antarctic phytoplankton aggregates and zooplankton faecal pellets sink rapidly (Asper and Smith, 2003; Pauli et al., 2021). Given the relatively shallow depth of the sills, phytoplankton-derived organic matter could reach the benthos within hours to less than a day, making substantial $\delta^{15}N$ alteration during vertical transit unlikely. Both shifts may partially explain the observed improvement in nutritional condition. Supporting this, Bascur et al. (2020) reported that *N. inaequisculpta* individuals of similar size at the sill station had nearly twice the soft tissue biomass compared to the others, and indicated that the sill could also act as a food retainer.

In Sheldon Cove, the sill at SC2 increased the $\delta^{15}N$ values in the anemone compared with those at a neighbouring station. Notably, SC2 also corresponds to the peak of dissolved oxygen concentrations within the fjord, suggesting relatively more ventilated near-bottom conditions at the sill. However, the trophic shift did not appear to translate into improved nutritional condition, as indicated by the constancy of C:N ratios. These findings indicate that the ecological effects of seabed morphology are context-dependent and could be shaped by local environmental conditions and species-specific biology.

4.6. Limitations of the study and future perspectives

This study has some limitations to consider when interpreting the results. First, potential food sources were not directly sampled, limiting our ability to explicitly link consumer isotopic signals with those of their potential prey. Second, the number of specimens per station was limited. Considering our sampling depths and the benthic patchy distribution observed in WAP glacier-influenced fjords (Pasotti et al., 2015a), analysing a larger sampling size of the same species across the entire fjord transect would be highly challenging. Despite this constraint, the number of specimens we used was sufficient to detect strong patterns and achieve the objectives.

Our work provides a baseline linking ^{13}C enrichment in polar benthic invertebrates to phytoplankton blooms in glacier-influenced fjords. Further analyses across other fjords along the WAP, encompassing additional taxa and feeding strategies, would provide valuable comparative insights. From this baseline, more integrative food-web studies could be conducted to elucidate how these species interact in recently deglaciated habitats. Future work could also aim to establish temporal isotopic datasets to track ecological responses over time. Such long-term observations would strengthen our ability to evaluate ecosystem trajectories and detect gradual shifts in benthic functioning as Antarctic glaciers continue to retreat. Additionally, reproductive traits in benthic invertebrates (e.g., gonad development, fecundity, egg size; Lau et al., 2018) could be studied across glacier-influenced fjords. Such approaches may help to determine whether the likely food scarcity near glacier fronts (e.g., in Marian Cove) limits reproductive output.

5. Conclusion

This study provides some of the first evidence of stable isotope variation in benthic fauna along Antarctic glacier-influenced fjords. $\delta^{13}C$ tracked local phytoplankton productivity rather than simple proximity to the glacier within each fjord studied, pointing to primary production (and the environmental conditions that govern it) as the proximate driver of carbon signals in benthic consumers. $\delta^{15}N$, $\delta^{34}S$ and C:N ratios responded instead to finer-scale heterogeneity. Among local modulators, submarine sills stood out as geomorphological features associated with shifts in nutritional condition in the bivalve and in trophic level in the anemone. Low $\delta^{34}S$ values in both species further indicate that suboxic sediments are a pervasive feature of these glacier-influenced fjords, with potential consequences for baseline $\delta^{15}N$ and for consumer nutritional condition.

Beyond the specific patterns, two broader implications emerge. First, our results challenge the assumption that newly deglaciated fjord areas act as straightforward contributors to a negative climate change feedback in Antarctic benthic systems. Where surface meltwater suppresses primary production, the delivery of organic matter to the seafloor may be reduced, as reflected in the $\delta^{13}C$ signal of the bivalve near the land-terminating glacier at Marian Cove. Thus, the role of newly ice-free areas as carbon sinks likely depends on glacier configuration and associated meltwater dynamics. Second, $\delta^{34}S$ proves to be a particularly informative tracer in Antarctic benthic habitats, valuable both as a proxy for comparing sediment redox conditions and as a marker of baseline shifts affecting other isotopes. Future studies could also explore food webs, long-term variability, and reproductive effects, thereby complementing our work on how benthic invertebrates are influenced by modified ecosystem functioning under continued Antarctic glacier retreat.

CRediT authorship contribution statement

Pau Bardi-Puigdefàbregas: Conceptualization, Data curation, Formal analysis, Investigation, Methodology, Software, Validation, Visualization, Writing – original draft, Writing – review & editing. **Miguel Bascur:** Conceptualization, Formal analysis, Investigation, Methodology, Supervision, Validation, Visualization, Writing – review & editing. **David K.A. Barnes:** Funding acquisition, Investigation, Project administration, Resources, Supervision, Writing – review & editing. **Stuart Jenkins:** Funding acquisition, Investigation, Project administration, Resources, Supervision, Writing – review & editing. **Carlos P. Muñoz-Ramírez:** Investigation, Writing – review & editing. **Estefanía Rodríguez:** Investigation, Writing – review & editing. **Antonio Brante:** Funding acquisition, Investigation, Project administration, Resources, Writing – review & editing. **Luis Cardona:** Investigation, Methodology, Supervision, Validation, Writing – review & editing. **Conxita Avila:** Conceptualization, Investigation, Project administration, Resources, Supervision, Validation, Visualization, Writing – review & editing.

Declaration of generative AI use

During the preparation of this work, the authors used ChatGPT (OpenAI) and Grammarly to improve language clarity. After using these tools, the authors reviewed and edited the content as needed and take full responsibility for the content of the published article.

Funding

Financial support for the Antarctic expedition was provided by the Comisión Nacional de Investigación Científica y Tecnológica/Agencia Nacional de Investigación y Desarrollo (CONICYT/ANID), Chile, and the Natural Environment Research Council, UK, through the ICEBERGS project (PII20150078), awarded to A. B., D. B., and S. J. Sample shipment and laboratory analyses were funded by the projects CHALLENGE (PID2019-107979RB-I00, funded by MICIU/AEI/10.13039/501100011033) and CHALLENGE-2 (PID2022-141628NB-I00, funded by MICIU/AEI/10.13039/501100011033), from the Spanish Government and the European Regional Development Fund, awarded to C. A. Additional support was provided by the 'Marine Biodiversity and Evolution' (2021SGR01271) Research Quality Group funding programme of the Generalitat de Catalunya, Spain. M. B. acknowledges financial support from ANID, through the Becas Chile de Doctorado en el Extranjero programme (folio 72220140).

Declaration of competing interest

The authors declare that they have no known competing financial interests or personal relationships that could have appeared to influence the work reported in this paper.

Acknowledgements

We thank the crew and scientific members involved in the 2018 ICEBERGS II Antarctic campaign, on board the RRS James Clark Ross. We appreciate the support of the staff of the Centres Científics i Tecnològics of the Universitat de Barcelona with the stable isotope analysis. We are also grateful to Dr Rhiannon L. Jones for her valuable advice on the interpretation of environmental data, and to Dr Alessandra Cani for her support with the isotope work. We also thank the reviewer and the handling editor for their comments, which helped improve the manuscript. This study is a contribution to the 'Integrated Science to Inform Antarctic and Southern Ocean Conservation' research programme, supported by the Scientific Committee on Antarctic Research. P.B.P. would like to dedicate this work to his grandmother Francis, in gratitude for the privilege of learning from her example.

Appendix A. Supplementary data

Supplementary data to this article can be found online at https://doi.org/10.1016/j.marenvres.2026.108123.

Data availability

The datasets generated during the current study are available in Mendeley Data: Stable isotope data of two benthic invertebrates and environmental variables from Marian and Sheldon Coves (Western Antarctic Peninsula) (Original data).

References

Alderkamp, A.-C., Mills, M.M., Van Dijken, G.L., Laan, P., Thuróczy, C.-E., Gerringa, L.J. A., De Baar, H.J.W., Payne, C.D., Visser, R.J.W., Buma, A.G.J., Arrigo, K.R., 2012. Iron from melting glaciers fuels phytoplankton blooms in the Amundsen Sea (Southern Ocean): Phytoplankton characteristics and productivity. Deep Sea Res. Part II Top. Stud. Oceanogr. 71–76, 32–48. https://doi.org/10.1016/j.dsr2.2012.03.005.

Alley, R.B., Cuffey, K.M., Bassis, J.N., Alley, K.E., Wang, S., Parizek, B.R., Anandakrishnan, S., Christianson, K., DeConto, R.M., 2023. Iceberg calving: regimes and transitions. Annu. Rev. Earth Planet Sci. 51, 189–215. https://doi.org/10.1146/annurev-earth-032320-110916.

Altabet, M.A., 2007. Constraints on oceanic N balance/imbalance from sedimentary ^{15}N records. Biogeosciences 4, 75–86. https://doi.org/10.5194/bg-4-75-2007.

Alurralde, G., Fuentes, V.L., De Troch, M., Tatián, M., 2020. Suspension feeders as natural sentinels of the spatial variability in food sources in an antarctic fjord: a stable isotope approach. Ecol. Indic. 115, 106378. https://doi.org/10.1016/j.ecolind.2020.106378.

Alurralde, G., Fuentes, V.L., Maggioni, T., Movilla, J., Olariaga, A., Orejas, C., Schloss, I. R., Tatián, M., 2019. Role of suspension feeders in Antarctic pelagic-benthic coupling: trophic ecology and potential carbon sinks under climate change. Mar. Environ. Res. 152, 104790. https://doi.org/10.1016/j.marenvres.2019.104790.

Amiraux, R., Mundy, C.J., Pierrejean, M., Niemi, A., Hedges, K.J., Brown, T.A., Ehn, J.K., Elliott, K.H., Ferguson, S.H., Fisk, A.T., Gilchrist, G., Harris, L.N., Iken, K., Jacobs, K. B., Johnson, K.F., Kuzyk, Z.A., Limoges, A., Loewen, T.N., Love, O.P., Matthews, C.J. D., Ogloff, W.R., Rosenberg, B., Søreide, J.E., Watt, C.A., Yurkowski, D.J., 2023. Tracing carbon flow and trophic structure of a coastal arctic marine food web using highly branched isoprenoids and carbon, nitrogen and sulfur stable isotopes. Ecol. Indic. 147, 109938. https://doi.org/10.1016/j.ecolind.2023.109938.

Annett, A.L., Skiba, M., Henley, S.F., Venables, H.J., Meredith, M.P., Statham, P.J., Ganeshram, R.S., 2015. Comparative roles of upwelling and glacial iron sources in Ryder Bay, coastal Western Antarctic Peninsula. Mar. Chem. 176, 21–33. https://doi.org/10.1016/j.marchem.2015.06.017.

Asper, V.L., Smith, W.O., 2003. Abundance, distribution and sinking rates of aggregates in the Ross Sea, Antarctica. Deep-Sea Res. I: Oceanogr. Res. Pap. 50, 131–150. https://doi.org/10.1016/S0967-0637(02)00146-2.

Bae, H., Ahn, I.-Y., Park, J., Song, S.J., Noh, J., Kim, H., Khim, J.S., 2021. Shift in polar benthic community structure in a fast retreating glacial area of marian cove, West Antarctica. Sci. Rep. 11, 241. https://doi.org/10.1038/s41598-020-80636-z.

Barnes, D.K.A., 2017. Iceberg killing fields limit huge potential for benthic blue carbon in Antarctic shallows. Glob. Change Biol. 23, 2649–2659. https://doi.org/10.1111/gcb.13523.

Barnes, D.K.A., Sands, C.J., Cook, A., Howard, F., Román-González, A., Muñoz–Ramirez, C., Retallick, K., Scourse, J.D., Van Landeghem, K., Zwerschke, N., 2020. Blue carbon gains from glacial retreat along antarctic fjords: what should we expect? Glob. Change Biol. 26, 2750–2755. https://doi.org/10.1111/gcb.15055.

Barnes, D.K.A., Sands, C.J., 2017. Functional group diversity is key to Southern Ocean benthic carbon pathways. PLoS One 12, e0179735. https://doi.org/10.1371/journal.pone.0179735.

Bas, M., Cardona, L., 2018. Effects of skeletal element identity, delipidation and demineralization on the analysis of stable isotope ratios of C and N in fish bone. J. Fish. Biol. 92, 420–437. https://doi.org/10.1111/jfb.13521.

Bascur, M., Muñoz-Ramírez, C., Román-González, A., Sheen, K., Barnes, D.K.A., Sands, C. J., Brante, A., Urzúa, Á., 2020. The influence of glacial melt and retreat on the nutritional condition of the bivalve *Nuculana inaequisculpta* (Protobranchia: Nuculanidae) in the West Antarctic Peninsula. PLoS One 15, e0233513. https://doi.org/10.1371/journal.pone.0233513.

Björk, G., Nordberg, K., Arneborg, L., Bornmalm, L., Harland, R., Robijn, A., Ödalen, M., 2017. Seasonal oxygen depletion in a shallow sill fjord on the Swedish west coast. J. Mar. Syst. 175, 1–14. https://doi.org/10.1016/j.jmarsys.2017.06.004.

Boecklen, W.J., Yarnes, C.T., Cook, B.A., James, A.C., 2011. On the use of stable isotopes in trophic ecology. Annu. Rev. Ecol. Evol. Syst. 42, 411–440. https://doi.org/10.1146/annurev-ecolsys-102209-144726.

Bond, A.L., Hobson, K.A., 2012. Reporting stable-isotope ratios in ecology: recommended terminology, guidelines and best practices. Waterbirds 35, 324. https://doi.org/10.1675/063.035.0213.

Bown, J., Laan, P., Ossebaar, S., Bakker, K., Rozema, P., De Baar, H.J.W., 2017. Bioactive trace metal time series during Austral summer in Ryder Bay, Western Antarctic Peninsula. Deep Sea Res. Part II Top. Stud. Oceanogr. 139, 103–119. https://doi.org/10.1016/j.dsr2.2016.07.004.

Breusch, T.S., Pagan, A.R., 1979. A simple test for heteroscedasticity and random coefficient variation. Econometrica 47, 1287–1294. https://doi.org/10.2307/1911963.

Burnham, K.P., Anderson, D.R., 2004. Model Selection and Multimodel Inference, second ed. Springer, New York. https://doi.org/10.1007/b97636.

Canfield, D.E., 2001. Isotope fractionation by natural populations of sulfate-reducing bacteria. Geochem. Cosmochim. Acta 65, 1117–1124. https://doi.org/10.1016/S0016-7037(00)00584-6.

Cani, A., Besén, C., Carreras, C., Pascual, M., Cardona, L., 2025. The journey of loggerhead turtles from the Northwest Atlantic to the Mediterranean Sea as recorded by the stable isotope ratios of O, C and N of their bones. Mar. Environ. Res. 203, 106851. https://doi.org/10.1016/j.marenvres.2024.106851.

Cardona, L., Lloret-Lloret, E., Moles, J., Avila, C., 2021. Latitudinal changes in the trophic structure of benthic coastal food webs along the Antarctic peninsula. Mar. Environ. Res. 167, 105290. https://doi.org/10.1016/j.marenvres.2021.105290.

Cattaneo-Vietti, R., Chiantore, M., Schiaparelli, S., Albertelli, G., 2000. Shallow- and deep-water mollusc distribution at Terra Nova Bay (Ross Sea, Antarctica). Polar Biol. 23, 173–182. https://doi.org/10.1007/s003000050024.

Choy, E.J., Park, H., Kim, J.-H., Ahn, I.-Y., Kang, C.-K., 2011. Isotopic shift for defining habitat exploitation by the antarctic limpet *Nacella concinna* from rocky coastal habitats (Marian Cove, King George Island). Estuar. Coast Shelf Sci. 92, 339–346. https://doi.org/10.1016/j.ecss.2011.01.009.

Clarke, A., Murphy, E.J., Meredith, M.P., King, J.C., Peck, L.S., Barnes, D.K.A., Smith, R. C., 2007. Climate change and the marine ecosystem of the western Antarctic Peninsula. Philos. Trans. R. Soc. B 362, 149–166. https://doi.org/10.1098/rstb.2006.1958.

Convey, P., Peck, L.S., 2019. Antarctic environmental change and biological responses. Sci. Adv. 5. https://doi.org/10.1126/sciadv.aaz0888 eaaz0888.

Cook, A.J., Holland, P.R., Meredith, M.P., Murray, T., Luckman, A., Vaughan, D.G., 2016. Ocean forcing of glacier retreat in the western Antarctic Peninsula. Science 353, 283–286. https://doi.org/10.1126/science.aae0017.

Corbisier, T.N., Bromberg, S., Gheller, P.F., Elias-Piera, F., Petti, M.A.V., 2010. Monitoring the impact of human activities in Admiralty Bay, King George Island, Antarctica: isotopic analysis of C and N in the summer of 2005/2006. INCT-APA Annual Activity Report 181–187. https://doi.org/10.4322/apa.2014.047.

Corbisier, T.N., Petti, M.A.V., Skowronski, R.S.P., Brito, T.A.S., 2004. Trophic relationships in the nearshore zone of Martel Inlet (King George Island, Antarctica): $\delta^{13}C$ stable-isotope analysis. Polar Biol. 27, 75–82. https://doi.org/10.1007/s00300-003-0567-z.

Dalerum, F., Angerbjörn, A., 2005. Resolving temporal variation in vertebrate diets using naturally occurring stable isotopes. Oecologia 144, 647–658. https://doi.org/10.1007/s00442-005-0118-0.

Daly, M., Perissinotto, R., Laird, M., Dyer, D., Todaro, A., 2012. Description and ecology of a new species of *Edwardsia* de Quatrefages, 1842 (Anthozoa, Actiniaria) from the St Lucia Estuary, South Africa. Mar. Biol. Res. 8, 233–245. https://doi.org/10.1080/17451000.2011.617757.

Davenport, J., 1988. The feeding mechanism of *Yoldia* (= *Aequiyoldia) eightsi* (Courthouy). Proc. Roy. Soc. Lond. B. 232, 431–442. https://doi.org/10.1098/rspb.1988.0005.

Demidov, A.B., Artemiev, V.A., Polukhin, A.A., Flint, M.V., Eremeeva, E.V., 2023. Influence of land-terminating glacier on primary production in the high Arctic fjord (Blagopoluchiya Bay, Novaya Zemlya archipelago, Kara Sea). Estuar. Coast Shelf Sci. 292, 108468. https://doi.org/10.1016/j.ecss.2023.108468.

Dunton, K.H., 2001. $\delta^{15}N$ and $\delta^{13}C$ measurements of Antarctic Peninsula fauna: Trophic relationshipt and assimilation of benthic seaweeds. Am. Zool. 41, 99–112. https://doi.org/10.1093/icb/41.1.99.

Elias-Piera, F., 2015. Biomarkers of bentho-pelagic coupling in Antarctica a spatio-temporal comparison in the Weddell Sea. Doctoral dissertation. Universitat Autònoma de Barcelona, Barcelona. https://ddd.uab.cat/record/129020.

Engl, W., 2012. Shells of Antarctica, first ed. ConchBooks, Hackenheim.

Fox, J., 1991. Regression Diagnostics, first ed. Sage, Newbury Park. https://doi.org/10.4135/9781412985604.

Fox, J., Weisberg, S., Price, B., 2024. Car: companion to applied regression. v3.1-v3.3 [software]. https://doi.org/10.32614/CRAN.package.car.

Fraser, M.R., Walker, T.R., Sherwood, O.A., Oakes, K.D., 2024. Assessing spatial impacts of historical pulp mill effluent on trophic dynamics in a coastal marine ecosystem using stable isotope ($\delta^{13}C$ and $\delta^{15}N$) analysis. Mar. Pollut. Bull. 198, 115859. https://doi.org/10.1016/j.marpolbul.2023.115859.

Fry, B., Cox, J., Gest, H., Hayes, J.M., 1986. Discrimination between ^{34}S and ^{32}S during bacterial metabolism of inorganic sulfur compounds. J. Bacteriol. 165, 328–330. https://doi.org/10.1128/jb.165.1.328-330.1986.

Games, P.A., Howell, J.F., 1976. Pairwise multiple comparison procedures with unequal N's and/or variances: a Monte Carlo Study. J. Educ. Stat. 1, 113–125. https://doi.org/10.2307/1164979.

Gastwirth, J.L., Gel, Y.R., Miao, W., 2009. The impact of Levene's test of equality of variances on statistical theory and practice. Stat. Sci. 24, 343–360. https://doi.org/10.1214/09-STS301.

Gillies, C., Stark, J., Johnstone, G., Smith, S., 2013. Establishing a food web model for coastal Antarctic benthic communities: a case study from the Vestfold hills. Mar. Ecol. Prog. Ser. 478, 27–41. https://doi.org/10.3354/meps10214.

Gillies, C.L., Stark, J.S., Johnstone, G.J., Smith, S.D.A., 2012. Carbon flow and trophic structure of an Antarctic coastal benthic community as determined by $\delta^{13}C$ and $\delta^{15}N$. Estuar. Coast Shelf Sci. 97, 44–57. https://doi.org/10.1016/j.ecss.2011.11.003.

Goeyens, L., Tréguer, P., Baumann, M.E.M., Baeyens, W., Dehairs, F., 1995. The leading role of ammonium in the nitrogen uptake regime of Southern Ocean marginal ice zones. J. Mar. Syst. 6, 345–361. https://doi.org/10.1016/0924-7963(94)00033-8.

Gordillo, S., Malvé, M.E., Moran, G., 2017. Benthic mollusc assemblages in West Antarctica: taxa composition and ecological insights. Mar. Freshw. Res. 68, 2095. https://doi.org/10.1071/MF16349.

Grange, L.J., Smith, C.R., 2013. Megafaunal communities in rapidly warming fjords along the west Antarctic Peninsula: hotspots of abundance and beta diversity. PLoS One 8, e77917. https://doi.org/10.1371/journal.pone.0077917.

Hodson, A., Nowak, A., Sabacka, M., Jungblut, A., Navarro, F., Pearce, D., Ávila-Jiménez, M.L., Convey, P., Vieira, G., 2017. Climatically sensitive transfer of iron to maritime Antarctic ecosystems by surface runoff. Nat. Commun. 8, 14499. https://doi.org/10.1038/ncomms14499.

Hoefs, J., 2021. Stable isotope geochemistry. Springer Textbooks in Earth Sciences, Geography and Environment, ninth ed. Springer, Cham. https://doi.org/10.1007/978-3-030-77692-3.

Holding, J.M., Markager, S., Juul-Pedersen, T., Paulsen, M.L., Møller, E.F., Meire, L., Sejr, M.K., 2019. Seasonal and spatial patterns of primary production in a high-latitude fjord affected by Greenland Ice Sheet run-off. Biogeosciences 16, 3777–3792. https://doi.org/10.5194/bg-16-3777-2019.

Holdsworth, G., Glynn, J.E., 1981. A mechanism for the formation of large icebergs. J. Geophys. Res. 86, 3210–3222. https://doi.org/10.1029/JC086iC04p03210.

Hoshiba, Y., Matsumura, Y., Kanna, N., Ohashi, Y., Sugiyama, S., 2024. Impacts of glacial discharge on the primary production in a Greenlandic fjord. Sci. Rep. 14, 15530. https://doi.org/10.1038/s41598-024-64529-z.

Hothorn, T., Zeileis, A., Farebrother, R.W., Cummins, C., 2022. Lmtest: testing linear regression models. v0.9-40 [software]. https://doi.org/10.32614/CRAN.package.lmtest.

Iken, K., Amsler, C.D., Gorman, K.B., Klein, A.G., Galloway, A.W.E., Amsler, M.O., Heiser, S., Whippo, R., Lowe, A.T., Schram, J.B., Schneider, Z.X., McClintock, J.B., 2023. Macroalgal input into the coastal food web along a gradient of seasonal sea ice cover along the Western Antarctic Peninsula. Mar. Ecol. Prog. Ser. 718, 1–22. https://doi.org/10.3354/meps14388.

Iken, K., Brey, T., Wand, U., Voigt, J., Junghans, P., 2001. Food web structure of the benthic community at the porcupine abyssal plain (NE Atlantic): a stable isotope analysis. Prog. Oceanogr. 50, 383–405. https://doi.org/10.1016/S0079-6611(01)00062-3.

Javornik, J., Hopkins, J.B.I.I.I., Zayadlay, S., Levanič, T., Lojen, S., Polak, Jerina, K., 2019. Effects of ethanol storage and lipids on stable isotope values in a large mammalian omnivore. J. Mamal. 100, 150–157. https://doi.org/10.1093/jmammal/gyy187.

Jędruch, A., Ziółkowska, M., Bulik, N., Paneth, P., Korejwo, E., Saniewska, D., 2025. Factors influencing the variability of stable isotopes of carbon, nitrogen, and sulfur in benthic macrofauna from Admiralty Bay, maritime Antarctic. Mar. Chem. 273, 104564. https://doi.org/10.1016/j.marchem.2025.104564.

Jones, R.L., Meredith, M.P., Lohan, M.C., Woodward, E.M.S., Van Landeghem, K., Retallick, K., Flanagan, O., Vora, M., Annett, A.L., 2023. Continued glacial retreat linked to changing macronutrient supply along the West Antarctic Peninsula. Mar. Chem. 251, 104230. https://doi.org/10.1016/j.marchem.2023.104230.

Kassambara, A., 2025. Rstatix: Pipe-friendly framework for basic statistical tests, v0.7.3 [software]. https://doi.org/10.32614/CRAN.package.rstatix.

Kim, B.K., Jeon, M., Joo, H.M., Kim, T.-W., Park, S.-J., Park, J., Ha, S.-Y., 2021. Impact of freshwater discharge on the carbon uptake rate of phytoplankton during summer (January–February 2019) in Marian Cove, King George Island, Antarctica. Front. Mar. Sci. 8, 725173. https://doi.org/10.3389/fmars.2021.725173.

Klages, J.P., Hillenbrand, C.-D., Bohaty, S.M., Salzmann, U., Bickert, T., Lohmann, G., Knahl, H.S., Gierz, P., Niu, L., Titschack, J., Kuhn, G., Frederichs, T., Müller, J., Bauersachs, T., Larter, R.D., Hochmuth, K., Ehrmann, W., Nehrke, G., Rodríguez-Tovar, F.J., Schmiedl, G., Spezzaferri, S., Läufer, A., Lisker, F., Van De Flierdt, T., Eisenhauer, A., Uenzelmann-Neben, G., Esper, O., Smith, J.A., Pälike, H., Spiegel, C., Dziadek, R., Ronge, T.A., Freudenthal, T., Gohl, K., 2024. Ice sheet–free West Antarctica during peak early Oligocene glaciation. Science 385, 322–327. https://doi.org/10.1126/science.adj3931.

Kuznetsova, A., Brockhoff, P.B., Christensen, R.H.B., 2020. lmerTest: tests in linear mixed effects models. v3.1-v3.3 [software]. https://doi.org/10.32614/CRAN.package.lmerTest.

Laird, N.M., Ware, J.H., 1982. Random-effects models for longitudinal data. Biometrics 38, 963. https://doi.org/10.2307/2529876.

Lamy, E., 1906. Sur quelques mollusques des Orcades du Sud. Bull. Mus. Hist. Nat. 12, 121–126.

Lau, S.C.Y., Grange, L.J., Peck, L.S., Reed, A.J., 2018. The reproductive ecology of the Antarctic bivalve *Aequiyoldia eightsii* (Protobranchia: sareptidae) follows neither Antarctic nor taxonomic patterns. Polar Biol. 41, 1693–1706. https://doi.org/10.1007/s00300-018-2309-2.

Lüdecke, D., Makowski, D., Ben-Shachar, M.S., Patil, I., Waggoner, P., Wiernik, B.M., Thériault, R., 2025. Performance: assessment of regression models performance, v0.15.2 [software]. https://doi.org/10.32614/CRAN.package.performance.

Le Bourg, B., Lepoint, G., Michel, L.N., 2019. Effects of preservation methodology on stable isotope compositions of sea stars. Rapid Commun. Mass Spectrom. 34, e8589. https://doi.org/10.1002/rcm.8589.

Lee, I.O., Noh, J., Bae, H., Kim, H., Kim, D.-U., Song, S.J., Ahn, I.-Y., Khim, J.S., 2025. Climate change-driven ice variability and isotopic polarization in Antarctic coastal food webs. Commun. Earth Environ. 6, 204. https://doi.org/10.1038/s43247-025-02163-x.

Levicoy, D., Flores, K., Rosenfeld, S., Cárdenas, L., 2021. Phylogeography and genetic diversity of the microbivalve *Kidderia subquadrata*, reveals new data from West Antarctic Peninsula. Sci. Rep. 11, 5705. https://doi.org/10.1038/s41598-021-85042-7.

Levin, L.A., Ekau, W., Gooday, A.J., Jorissen, F., Middelburg, J.J., Naqvi, S.W.A., Neira, C., Rabalais, N.N., Zhang, J., 2009. Effects of natural and human-induced hypoxia on coastal benthos. Biogeosciences 6, 2063–2098. https://doi.org/10.5194/bg-6-2063-2009.

Linse, K., Cope, T., Lörz, A.-N., Sands, C., 2007. Is the Scotia Sea a centre of Antarctic marine diversification? Some evidence of cryptic speciation in the circum-Antarctic bivalve *Lissarca notorcadensis* (Arcoidea: philobryidae). Polar Biol. 30, 1059–1068. https://doi.org/10.1007/s00300-007-0265-3.

Lovell, L.L., Trego, K.D., 2003. The epibenthic megafaunal and benthic infaunal invertebrates of Port Foster, Deception Island (South Shetland Islands, Antarctica). Deep Sea Res. Part II Top. Stud. Oceanogr. 50, 1799–1819. https://doi.org/10.1016/S0967-0645(03)00087-0.

Markovic, S., Paytan, A., Wortmann, U.G., 2015. Pleistocene sediment offloading and the global sulfur cycle. Biogeosciences 12, 3043–3060. https://doi.org/10.5194/bg-12-3043-2015.

Michel, L.N., Danis, B., Dubois, P., Eleaume, M., Fournier, J., Gallut, C., Jane, P., Lepoint, G., 2019. Increased sea ice cover alters food web structure in East Antarctica. Sci. Rep. 9, 8062. https://doi.org/10.1038/s41598-019-44605-5.

Mincks, S.L., Smith, C.R., Jeffreys, R.M., Sumida, P.Y.G., 2008. Trophic structure on the West Antarctic Peninsula shelf: detritivory and benthic inertia revealed by $\delta^{13}C$ and $\delta^{15}N$ analysis. Deep Sea Res. Part II Top. Stud. Oceanogr. 55, 2502–2514. https://doi.org/10.1016/j.dsr2.2008.06.009.

Moore, C.M., Mills, M.M., Arrigo, K.R., Berman-Frank, I., Bopp, L., Boyd, P.W., Galbraith, E.D., Geider, R.J., Guieu, C., Jaccard, S.L., Jickells, T.D., La Roche, J., Lenton, T.M., Mahowald, N.M., Marañón, E., Marinov, I., Moore, J.K., Nakatsuka, T., Oschlies, A., Saito, M.A., Thingstad, T.F., Tsuda, A., Ulloa, O., 2013. Processes and patterns of oceanic nutrient limitation. Nat. Geosci. 6, 701–710. https://doi.org/10.1038/ngeo1765.

Muñoz-Ramírez, C.P., Beltrán-Concha, M., Pérez-Araneda, K., Sands, C.J., Barnes, D.K.A., Román-González, A., De Lecea, A.M., Retallick, K., Van Landeghem, K., Sheen, K., Gonnelli, K., Scourse, J.D., Bascur, M., Brante, A., 2021. Genetic variation in the

small bivalve *Nuculana inaequisculpta* along a retreating glacier fjord, King George Island, Antarctica. Rev. Biol. Mar. Oceanogr. 56, 151–156. https://doi.org/10.22370/rbmo.2021.56.2.3059.
Muyzer, G., Stams, A.J.M., 2008. The ecology and biotechnology of sulphate-reducing bacteria. Nat. Rev. Microbiol. 6, 441–454. https://doi.org/10.1038/nrmicro1892.
Nakagawa, S., Schielzeth, H., 2010. Repeatability for Gaussian and non-gaussian data: a practical guide for biologists. Biol. Rev. 85, 935–956. https://doi.org/10.1111/j.1469-185X.2010.00141.x.
Oleszczuk, B., Silberberger, M.J., Grzelak, K., Winogradow, A., Dybwad, C., Peeken, I., Wiedmann, I., Kędra, M., 2023. Macrofauna and meiofauna food-web structure from Arctic fjords to deep Arctic Ocean during spring: a stable isotope approach. Ecol. Indic. 154, 110487. https://doi.org/10.1016/j.ecolind.2023.110487.
Ortiz, J.J., Preciado, I., Hidalgo, M., González-Irusta, J.M., Rabanal, I.M., López-López, L., 2024. Estimating spatial variability of baseline isoscapes from fish isotopic signatures at the community level. Prog. Oceanogr. 221, 103205. https://doi.org/10.1016/j.pocean.2024.103205.
Pasotti, F., Manini, E., Giovannelli, D., Wölfl, A., Monien, D., Verleyen, E., Braeckman, U., Abele, D., Vanreusel, A., 2015a. Antarctic shallow water benthos in an area of recent rapid glacier retreat. Mar. Ecol. 36, 716–733. https://doi.org/10.1111/maec.12179.
Pasotti, F., Saravia, L.A., De Troch, M., Tarantelli, M.S., Sahade, R., Vanreusel, A., 2015b. Benthic trophic interactions in an Antarctic shallow water ecosystem affected by recent glacier retreat. PLoS One 10, e0141742. https://doi.org/10.1371/journal.pone.0141742.
Pauli, N.C., Flintrop, C.M., Konrad, C., Pakhomov, E.A., Swoboda, S., Koch, F., Wang, X.-L., Zhang, J.-C., Brierley, A.S., Bernasconi, M., Meyer, B., Iversen, M.H., 2021. Krill and salp faecal pellets contribute equally to the carbon flux at the Antarctic Peninsula. Nat. Commun. 12, 7168. https://doi.org/10.1038/s41467-021-27436-9.
Peck, L.S., Barnes, D.K.A., Cook, A.J., Fleming, A.H., Clarke, A., 2010. Negative feedback in the cold: ice retreat produces new carbon sinks in Antarctica. Glob. Change Biol. 16, 2614–2623. https://doi.org/10.1111/j.1365-2486.2009.02071.x.
Peterson, B.J., 1999. Stable isotopes as tracers of organic matter input and transfer in benthic food webs: a review. Acta Oecol. 20, 479–487. https://doi.org/10.1016/S1146-609X(99)00120-4.
Peterson, B.J., Fry, B., 1987. Stable isotopes in ecosystem studies. Annu. Rev. Ecol. Systemat. 18, 293–320. https://doi.org/10.1146/annurev.es.18.110187.001453.
Pinheiro, J.C., Bates, D.M., 2000. Mixed-effects models in S and S-PLUS. Statistics and Computing, first ed. Springer, New York. https://doi.org/10.1007/b98882.
Pinheiro, J.C., Bates, D.M., R Core Team, 2025. Nlme: Linear and nonlinear mixed effects models. v3.1-168 [software]. https://doi.org/10.32614/CRAN.package.nlme.
Post, D.M., Layman, C.A., Arrington, D.A., Takimoto, G., Quattrochi, J., Montaña, C.G., 2007. Getting to the fat of the matter: models, methods and assumptions for dealing with lipids in stable isotope analyses. Oecologia 152, 179–189. https://doi.org/10.1007/s00442-006-0630-x.
Pratihary, A., Lavik, G., Naqvi, S.W.A., Shirodkar, G., Sarkar, A., Marchant, H., Ohde, T., Shenoy, D., Kurian, S., Uskaikar, H., Kuypers, M.M.M., 2023. Chemolithoautotrophic denitrification intensifies nitrogen loss in the eastern Arabian Sea Shelf waters during sulphidic events. Prog. Oceanogr. 217, 103075. https://doi.org/10.1016/j.pocean.2023.103075.
Quatrefages, A., 1842. Mémoire sur les Edwardsies (*Edwardsia* nob.) nouveau genre de la famille des actinies. Ann. Sci. Nat. 18, 65–109.
R Core Team, 2025. R: a Language and Environment for Statistical Computing, v4.5.1. R Foundation for Statistical Computing [software]. https://www.r-project.org/.
Raoult, V., Phillips, A.A., Nelson, J., Niella, Y., Skinner, C., Tilcock, M.B., Burke, P.J., Szpak, P., James, W.R., Harrod, C., 2024. Why aquatic scientists should use sulfur stable isotope ratios ($\delta^{34}S$) more often. Chemosphere 355, 141816. https://doi.org/10.1016/j.chemosphere.2024.141816.
Rau, G.H., Takahashi, T., Marais, D.J.D., 1989. Latitudinal variations in plankton $\delta^{13}C$: implications for CO_2 and productivity in past oceans. Nature 341, 516–518. https://doi.org/10.1038/341516a0.
Rodríguez, E., Barbeitos, M.S., Brugler, M.R., Crowley, L.M., Grajales, A., Gusmão, L., Häussermann, V., Reft, A., Daly, M., 2014. Hidden among sea anemones: the first comprehensive phylogenetic reconstruction of the order Actiniaria (Cnidaria, Anthozoa, Hexacorallia) reveals a novel group of hexacorals. PLoS One 9, e96998. https://doi.org/10.1371/journal.pone.0096998.
Rodríguez, E., Fautin, D., Daly, M., 2025. World list of actiniaria. World register of marine species. https://www.marinespecies.org/actiniaria. (Accessed 6 November 2025). https://doi.org/10.14284/568.
Ryan-Keogh, T.J., Thomalla, S.J., Mtshali, T.N., Little, H., 2017. Modelled estimates of spatial variability of iron stress in the Atlantic sector of the Southern Ocean. Biogeosciences 14, 3883–3897. https://doi.org/10.5194/bg-14-3883-2017.
Sahade, R., Lagger, C., Torre, L., Momo, F., Monien, P., Schloss, I., Barnes, D.K.A., Servetto, N., Tarantelli, S., Tatián, M., Zamboni, N., Abele, D., 2015. Climate change and glacier retreat drive shifts in an Antarctic benthic ecosystem. Sci. Adv. 1, e1500050. https://doi.org/10.1126/sciadv.1500050.
Sanamyan, N.P., Sanamyan, K.E., Schories, D., 2015. Shallow water Actiniaria and Corallimorpharia (Cnidaria: anthozoa) from King George Island, Antarctica. Invert. Zool. 12, 1–51. https://doi.org/10.15298/invertzool.12.1.01.
Sands, C.J., Annett, A., Apeland, B., Barnes, D.K.A., Bascur, M., Bruning, P., Costa, M., Dadd, G., De Lecea, A., Ensor, N., Featherstone, A., Flint, G., Goodger, D., Guzzi, A., Howard, F., Hunter, D., Jenkins, S., Kender, S., Lincoln, B., Muñoz-Ramírez, C., Pienkowski, A., Retallick, K., Román-González, A., Scourse, J.D., Sheen, K., Whitaker, T., Williams, J., Zhao, L., Zwerschke, N., 2018. Cruise Report RRS James Clark Ross JR18003. British Antarctic Survey, Cambridge.
Schwartz, C.C., Teisberg, J.E., Fortin, J.K., Haroldson, M.A., Servheen, C., Robbins, C.T., Van Manen, F.T., 2014. Use of isotopic sulfur to determine whitebark pine consumption by Yellowstone bears: a reassessment. Wildl. Soc. Bull. 38, 664–670. https://doi.org/10.1002/wsb.426.
Self, S.G., Liang, K.-Y., 1987. Asymptotic properties of maximum likelihood estimators and likelihood ratio tests under nonstandard conditions. J. Am. Stat. Assoc. 82, 605–610. https://doi.org/10.1080/01621459.1987.10478472.
Seyboth, E., Botta, S., Mendes, C.R.B., Negrete, J., Dalla Rosa, L., Secchi, E.R., 2018. Isotopic evidence of the effect of warming on the northern Antarctic Peninsula ecosystem. Deep Sea Res. Part II Top. Stud. Oceanogr. 149, 218–228. https://doi.org/10.1016/j.dsr2.2017.12.020.
Shapiro, S.S., Wilk, M.B., 1965. An analysis of variance test for normality (Complete Samples). Biometrika 52, 591–611. https://doi.org/10.2307/2333709.
Shrout, P.E., Fleiss, J.L., 1979. Intraclass correlations: uses in assessing rater reliability. Psychol. Bull. 86, 420–428. https://doi.org/10.1037/0033-2909.86.2.420.
Siegert, M., Atkinson, A., Banwell, A., Brandon, M., Convey, P., Davies, B., Downie, R., Edwards, T., Hubbard, B., Marshall, G., Rogelj, J., Rumble, J., Stroeve, J., Vaughan, D., 2019. The Antarctic Peninsula under a 1.5°C global warming scenario. Front. Environ. Sci. 7, 102. https://doi.org/10.3389/fenvs.2019.00102.
Silva, N., Vargas, C.A., 2014. Hypoxia in Chilean Patagonian fjords. Prog. Oceanogr. 129, 62–74. https://doi.org/10.1016/j.pocean.2014.05.016.
Simmons, N.E., Barnes, D.K.A., Scourse, J.D., Whitaker, J.M., Garza, T.N., Janosik, A.M., 2025. Quantifying microplastics concentration of invertebrates from three Antarctic fjords. Mar. Pollut. Bull. 212, 117503. https://doi.org/10.1016/j.marpolbul.2024.117503.
Skrzypek, G., 2013. Normalization procedures and reference material selection in stable HCNOS isotope analyses: an overview. Anal. Bioanal. Chem. 405, 2815–2823. https://doi.org/10.1007/s00216-012-6517-2.
Smith, R.W., Bianchi, T.S., Allison, M., Savage, C., Galy, V., 2015. High rates of organic carbon burial in fjord sediments globally. Nat. Geosci. 8, 450–453. https://doi.org/10.1038/ngeo2421.
Stark, J.S., Raymond, T., Deppeler, S.L., Morrison, A.K., 2019. Antarctic seas. In: Sheppard, C. (Ed.), World Seas: an Environmental Evaluation, second ed., vol. 3. Academic Press, London, pp. 1–44. https://doi.org/10.1016/B978-0-12-805068-2.00002-4.
Straneo, F., Cenedese, C., 2015. The dynamics of Greenland's glacial fjords and their role in climate. Ann. Rev. Mar. Sci 7, 89–112. https://doi.org/10.1146/annurev-marine-010213-135133.
Szpak, P., Buckley, M., 2020. Sulfur isotopes ($\delta^{34}S$) in Arctic marine mammals: indicators of benthic vs. pelagic foraging. Mar. Ecol. Prog. Ser. 653, 205–216. https://doi.org/10.3354/meps13493.
Thrush, S., Hewitt, J.E., Pilditch, C., Norkko, A., 2021. Ecology of coastal marine sediments: form, function. And Change in the Anthropocene, first ed. Oxford University Press, Oxford. https://doi.org/10.1093/oso/9780198804765.001.0001.
Tukey, J.W., 1949. Comparing individual means in the analysis of variance. Biometrics 5, 99–114. https://doi.org/10.2307/3001913.
Vander Zanden, M.J., Clayton, M.K., Moody, E.K., Solomon, C.T., Weidel, B.C., 2015. Stable isotope turnover and half-life in animal tissues: a literature synthesis. PLoS One 10, e0116182. https://doi.org/10.1371/journal.pone.0116182.
Vander Zanden, M.J., Rasmussen, J.B., 1999. Primary consumer $\delta^{13}C$ and $\delta^{15}N$ and the trophic position of aquatic consumers. Ecology 80, 1395–1404. https://doi.org/10.1890/0012-9658(1999)080%255B1395:PCCANA%255D2.0.CO;2.
Vaquer-Sunyer, R., Duarte, C.M., 2010. Sulfide exposure accelerates hypoxia-driven mortality. Limnol. Oceanogr. 55, 1075–1082. https://doi.org/10.4319/lo.2010.55.3.1075.
Wang, S., Li, G.-C., Zhang, Z.-H., Zhang, W.-Q., Wang, X., Chen, D., Chen, W., Ding, M.-H., 2025. Recent warming trends in Antarctica revealed by multiple reanalysis. Adv. Clim. Change Res. 16, 447–459. https://doi.org/10.1016/j.accre.2025.03.003.
Waser, N.A.D., Yin, K.D., Yu, Z.M., Tada, K., Harrison, P.J., Turpin, D.H., Calvert, S.E., 1998. Nitrogen isotope fractionation during nitrate, ammonium and urea uptake by marine diatoms and coccolithophores under various conditions of N availability. Mar. Ecol. Prog. Ser. 169, 29–41. https://doi.org/10.3354/meps169029.
Welch, B.L., 1951. On the comparison of several mean values: an alternative approach. Biometrika 38, 330–336. https://doi.org/10.2307/2332579.
Wood, S., 2025. Mgcv: mixed GAM computation vehicle with automatic smoothness estimation, v1.9-3 [software]. https://doi.org/10.32614/CRAN.package.mgcv.
Yakovis, E., Artemieva, A., Fokin, M., Varfolomeeva, M., 2012. Intraspecific variation in stable isotope signatures indicates no small-scale feeding interference between a horse mussel and an ascidian. Mar. Ecol. Prog. Ser. 467, 113–120. https://doi.org/10.3354/meps09951.
Zar, J.H., 2010. Biostatistical Analysis, fifth ed. Prentice-Hall/Pearson, Upper Saddle River.
Zardus, J.D., 2002. Protobranch bivalves. Adv. Mar. Biol. 42, 1–65. https://doi.org/10.1016/S0065-2881(02)42012-3.
Zettler, M.L., Bick, A., 2025. Molluscs from a shallow bay of King George Island (Antarctica, South Shetland Islands): an annotated checklist with new distributional records. Zootaxa 5631, 401–450. https://doi.org/10.11646/zootaxa.5631.3.1.
Zuur, A.F., Ieno, E.N., Elphick, C.S., 2010. A protocol for data exploration to avoid common statistical problems: *data exploration*. Methods Ecol. Evol. 1, 3–14. https://doi.org/10.1111/j.2041-210X.2009.00001.x.
Zuur, A.F., Ieno, E.N., Walker, N., Saveliev, A.A., Smith, G.M., 2009. Mixed effects models and extensions in ecology with R. Statistics for Biology and Health, first ed. Springer, New York. https://doi.org/10.1007/978-0-387-87458-6.
Zwerschke, N., Sands, C.J., Román-González, A., Barnes, D.K.A., Guzzi, A., Jenkins, S., Muñoz-Ramírez, C., Scourse, J.D., 2022. Quantification of blue carbon pathways contributing to negative feedback on climate change following glacier retreat in West Antarctic fjords. Glob. Change Biol. 28, 8–20. https://doi.org/10.1111/gcb.15898.